

Electronic supporting information for **Zr⁴⁺ Solution Structures from Pair Distribution Function Analysis**

Magnus Kløve,^a Rasmus Stubkjær Christensen,^a Ida Gjerlevsen Nielsen,^a Sanna Sommer,^a Mads Ry Vogel Jørgensen,^{a,b} Ann-Christin Dippel,^c and Bo Brummerstedt Iversen^{a*}

^a Center for Integrated Materials Research, Department of Chemistry and Interdisciplinary Nanoscience Center (iNANO), Aarhus University, Langelandsgade 140, DK-8000 Aarhus C, Denmark

^b MAX IV Laboratory, Lund University, Fotongatan 2, 225 94, Lund, Sweden

^c Deutsches Elektronen-Synchrotron DESY, D-22607 Hamburg, Germany

Contents

1. Fitting the PDF of ZrCl ₄ in water.....	3
1.1 Tables with refined parameters for tetramer models	4
2. Variation of concentration on aqueous ZrCl ₄ solutions	12
3. PDFs of dilute HCl solutions	14
4. Sample images of ZrCl ₄ pH series	14
5. Repetitions of aqueous zirconium solutions	16
6. Modelling of long-period modulation in PDF intensity in methanol and ethanol solutions of ZrCl ₄	17
7. Tables with refined parameters from fitting PDF of ZrCl ₄ in non-aqueous solutions.....	18
8. Repetition of methanol and ethanol ZrCl ₄ solutions	21
9. Experimental	24
9.1 Solution preparation.....	24
9.2 Total scattering experiments	24
9.3 Data treatment.....	25
9.4 PDF generation	26
References.....	54

1. Fitting the PDF of ZrCl₄ in water

Table S1. Model overview used for fitting the PDF of ZrCl₄ in water. All models are based on the [Zr₄(OH)₈(OH₂)₁₆]⁸⁺-tetramer with atomic positions derived from crystal structure of ZrOCl₂·8H₂O solved by Mak.¹ Input parameters and refined atomic positions can be seen in Tables S2-S9.

Model	Direct Cl coordination	Comments	Refined	Box dimensions	R _w
T1	÷		÷	-	0.411
T2	÷	Based on T1, but refined.	+	±0.1 Å	0.317
T3	÷	Based on T1, but refined.	+	±0.5 Å	0.277
T4	+		÷	-	0.449
T5	+	Based on T4, but refined.	+	±0.1 Å	0.232
T6	+	Based on T4, but refined.	+	±0.5 Å	0.199
T7	÷	Refined T5-model with all Cl atoms removed.	÷	-	0.339
T8 (final)	+	Refined T5-model + Cl–O distance as two-phase fit.	÷	-	0.204

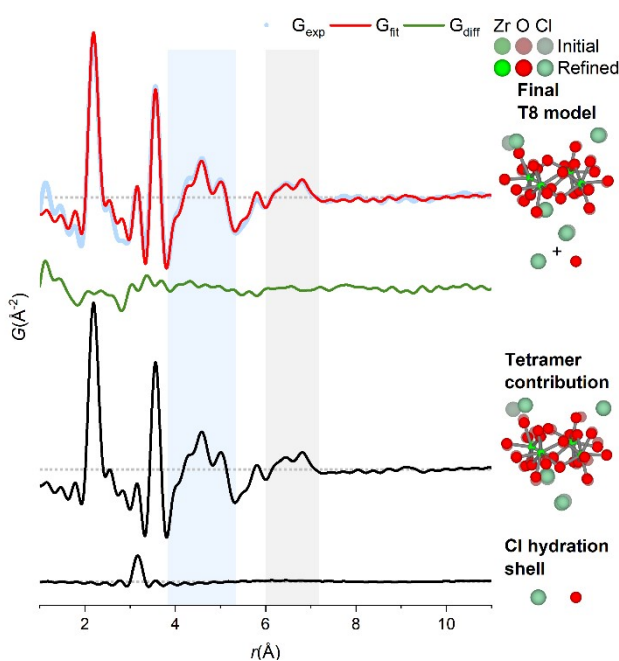


Figure S1. Partial PDFs of ZrCl₄ in water fitted with the two-phase **T8** tetramer model. Data collected at beamline P21.1@PETRA-III.

1.1 Tables with refined parameters for tetramer models

Table S2. Input parameters, R_w and atomic positions for fit of model T1 to the PDF of $ZrCl_4$ in water. The fit is a one-phase fit of the $[Zr_4(OH)_8(OH_2)_{16}]^{8+}$ -tetramer without direct chloride coordination. Hydrogen atoms are not included in the refinement. Atomic positions are not refined for this model.

T1 model			
Parameter	Value		
$B_{iso}(Zr) / \text{\AA}^2$	0.15		
$B_{iso}(O) / \text{\AA}^2$	0.15		
Q_{damp}	0.0483		
Q_{broad}	0.0174		
R_w	0.411		
Atom	x-coordinate	y-coordinate	z-coordinate
Zr(1)	8.054	11.021	3.889
Zr(2)	9.056	6.089	3.889
Zr(3)	6.089	8.054	3.821
Zr(4)	11.021	9.056	3.821
O(1)	7.251	9.431	2.722
O(2)	9.859	7.679	2.722
O(3)	7.679	7.251	4.988
O(4)	9.431	9.859	4.988
O(5)	8.055	11.927	6.044
O(6)	9.055	5.183	6.044
O(7)	5.183	8.055	1.666
O(8)	11.927	9.055	1.666
O(9)	6.281	12.338	3.953
O(10)	10.829	4.772	3.953
O(11)	4.772	6.281	3.757
O(12)	12.338	10.829	3.757
O(13)	4.192	9.212	3.867
O(14)	12.918	7.898	3.867
O(15)	7.898	4.192	3.843
O(16)	9.212	12.918	3.843
O(17)	6.630	9.758	4.986
O(18)	10.480	7.352	4.986
O(19)	7.352	6.630	2.724
O(20)	9.758	10.480	2.724
O(21)	7.741	11.903	1.773
O(22)	9.369	5.207	1.773
O(23)	5.207	7.741	5.937
O(24)	11.903	9.369	5.937

Table S3. Input parameters, R_w and refined atomic positions for fit of model **T2** to the PDF of $ZrCl_4$ in water. The fit is a one-phase fit of the $[Zr_4(OH)_8(OH_2)_{16}]^{8+}$ -tetramer without direct chloride coordination. Hydrogen atoms are not included in the refinement.

T2 model			
Parameter	Value		
$B_{iso}(Zr) / \text{\AA}^2$	0.15		
$B_{iso}(O) / \text{\AA}^2$	0.15		
$Box(Zr) / \text{\AA}$	± 0.1		
$Box(O) / \text{\AA}$	± 0.1		
Q_{damp}	0.0483		
Q_{broad}	0.0174		
R_w	0.317		
Atom	x-coordinate	y-coordinate	z-coordinate
Zr(1)	8.087	11.082	3.847
Zr(2)	9.078	6.063	3.941
Zr(3)	6.155	8.098	3.805
Zr(4)	11.021	9.056	3.821
O(1)	7.144	9.552	2.620
O(2)	9.966	7.570	2.702
O(3)	7.572	7.138	5.090
O(4)	9.532	9.970	5.015
O(5)	8.150	11.825	6.142
O(6)	8.961	5.283	6.145
O(7)	5.291	8.018	1.773
O(8)	11.820	9.106	1.774
O(9)	6.176	12.441	3.846
O(10)	10.933	4.670	3.847
O(11)	4.700	6.177	3.861
O(12)	12.439	10.725	3.860
O(13)	4.221	9.189	3.766
O(14)	12.956	8.003	3.764
O(15)	7.862	4.239	3.879
O(16)	9.200	13.013	3.946
O(17)	6.735	9.703	5.089
O(18)	10.374	7.440	5.088
O(19)	7.457	6.564	2.624
O(20)	9.702	10.373	2.620
O(21)	7.843	11.948	1.875
O(22)	9.269	5.243	1.878
O(23)	5.310	7.844	5.831
O(24)	11.800	9.267	5.833

Table S4. Input parameters, R_w and refined atomic positions for fit of model **T3** to the PDF of $ZrCl_4$ in water. The fit is a one-phase fit of the $[Zr_4(OH)_8(OH_2)_{16}]^{8+}$ -tetramer without direct chloride coordination. Hydrogen atoms are not included in the refinement.

T3 model			
Parameter	Value		
$B_{iso}(Zr) / \text{\AA}^2$	0.15		
$B_{iso}(O) / \text{\AA}^2$	0.15		
$Box(Zr) / \text{\AA}$	± 0.5		
$Box(O) / \text{\AA}$	± 0.5		
Q_{damp}	0.0483		
Q_{broad}	0.0174		
R_w	0.277		
Atom	x-coordinate	y-coordinate	z-coordinate
Zr(1)	8.060	11.064	3.862
Zr(2)	9.176	6.078	3.902
Zr(3)	6.173	8.025	3.764
Zr(4)	11.021	9.056	3.821
O(1)	6.799	9.782	2.594
O(2)	10.015	7.629	2.546
O(3)	7.691	6.975	5.191
O(4)	9.680	9.955	5.258
O(5)	8.079	11.743	5.912
O(6)	9.149	5.192	5.955
O(7)	5.614	8.172	1.705
O(8)	11.457	9.216	1.698
O(9)	6.228	12.708	3.530
O(10)	10.960	4.816	3.452
O(11)	4.783	6.382	4.181
O(12)	12.555	10.684	4.258
O(13)	3.811	9.255	3.367
O(14)	12.963	7.716	3.370
O(15)	8.044	4.039	4.343
O(16)	9.231	12.882	4.343
O(17)	6.560	9.864	4.792
O(18)	10.276	7.469	5.083
O(19)	7.530	6.699	2.664
O(20)	9.917	10.358	2.550
O(21)	7.404	11.937	1.973
O(22)	9.501	5.191	1.851
O(23)	5.272	7.763	5.740
O(24)	11.922	9.351	5.818

Table S5. Input parameters, R_w and atomic positions for fit of model **T4** to the PDF of $ZrCl_4$ in water. The fit is a one-phase fit of the $[Zr_4(OH)_8(OH_2)_{16}]^{8+}$ -tetramer with direct chloride coordination. Hydrogen atoms are not included in the refinement. Atomic positions are not refined for this model.

T4 model			
Parameter	Value		
$B_{iso}(Zr) / \text{\AA}^2$	0.15		
$B_{iso}(O) / \text{\AA}^2$	0.15		
$B_{iso}(Cl) / \text{\AA}^2$	0.15		
Q_{damp}	0.0483		
Q_{broad}	0.0174		
R_w	0.449		
Atom	x-coordinate	y-coordinate	z-coordinate
Zr(1)	8.054	11.021	3.889
Zr(2)	9.056	6.089	3.889
Zr(3)	6.089	8.054	3.821
Zr(4)	11.021	9.056	3.821
Cl(1)	5.306	10.831	0.238
Cl(2)	11.804	6.279	0.238
Cl(3)	6.279	5.306	7.472
Cl(4)	10.831	11.804	7.472
O(1)	7.251	9.431	2.722
O(2)	9.859	7.679	2.722
O(3)	7.679	7.251	4.988
O(4)	9.431	9.859	4.988
O(5)	8.055	11.927	6.044
O(6)	9.055	5.183	6.044
O(7)	5.183	8.055	1.666
O(8)	11.927	9.055	1.666
O(9)	6.281	12.338	3.953
O(10)	10.829	4.772	3.953
O(11)	4.772	6.281	3.757
O(12)	12.338	10.829	3.757
O(13)	4.192	9.212	3.867
O(14)	12.918	7.898	3.867
O(15)	7.898	4.192	3.843
O(16)	9.212	12.918	3.843
O(17)	6.630	9.758	4.986
O(18)	10.480	7.352	4.986
O(19)	7.352	6.630	2.724
O(20)	9.758	10.480	2.724
O(21)	7.741	11.903	1.773
O(22)	9.369	5.207	1.773
O(23)	5.207	7.741	5.937
O(24)	11.903	9.369	5.937

Table S6. Input parameters, R_w and refined atomic positions for fit of model **T5** to the PDF of $ZrCl_4$ in water. The fit is a one-phase fit of the $[Zr_4(OH)_8(OH_2)_{16}]^{8+}$ -tetramer with direct chloride coordination. Hydrogen atoms are not included in the refinement.

T5 model			
Parameter	Value		
$B_{iso}(Zr) / \text{\AA}^2$	0.15		
$B_{iso}(O) / \text{\AA}^2$	0.15		
$B_{iso}(Cl) / \text{\AA}^2$	0.15		
$Box(Zr) / \text{\AA}$	± 0.1		
$Box(O) / \text{\AA}$	± 0.1		
$Box(Cl) / \text{\AA}$	± 2		
Q_{damp}	0.0483		
Q_{broad}	0.0174		
R_w	0.232		
Atom	x-coordinate	y-coordinate	z-coordinate
Zr(1)	8.074	11.004	3.990
Zr(2)	9.126	6.030	3.994
Zr(3)	6.152	8.011	3.764
Zr(4)	11.021	9.056	3.821
Cl(1)	5.169	10.994	0.161
Cl(2)	11.398	6.517	-0.003
Cl(3)	6.665	5.805	7.580
Cl(4)	10.782	11.674	7.483
O(1)	7.146	9.539	2.641
O(2)	9.962	7.574	2.629
O(3)	7.684	7.222	4.979
O(4)	9.538	9.962	5.092
O(5)	8.017	11.826	5.988
O(6)	9.161	5.081	5.938
O(7)	5.284	8.158	1.564
O(8)	11.826	9.096	1.767
O(9)	6.176	12.438	3.850
O(10)	10.931	4.754	3.852
O(11)	4.873	6.181	3.859
O(12)	12.430	10.934	3.859
O(13)	4.187	9.313	3.969
O(14)	12.890	7.863	3.786
O(15)	7.873	4.258	3.801
O(16)	9.254	12.819	3.742
O(17)	6.732	9.655	5.073
O(18)	10.373	7.456	5.087
O(19)	7.454	6.527	2.824
O(20)	9.654	10.377	2.678
O(21)	7.734	11.802	1.856
O(22)	9.267	5.174	1.875
O(23)	5.104	7.845	5.832
O(24)	11.929	9.266	5.834

Table S7. Input parameters, R_w and refined atomic positions for fit of model **T6** to the PDF of $ZrCl_4$ in water. The fit is a one-phase fit of the $[Zr_4(OH)_8(OH_2)_{16}]^{8+}$ -tetramer with direct chloride coordination. Hydrogen atoms are not included in the refinement.

T6 model			
Parameter	Value		
$B_{iso}(Zr) / \text{\AA}^2$	0.15		
$B_{iso}(O) / \text{\AA}^2$	0.15		
$B_{iso}(Cl) / \text{\AA}^2$	0.15		
$Box(Zr) / \text{\AA}$	± 0.5		
$Box(O) / \text{\AA}$	± 0.5		
$Box(Cl) / \text{\AA}$	± 2		
Q_{damp}	0.0483		
Q_{broad}	0.0174		
R_w	0.199		
Atom	x-coordinate	y-coordinate	z-coordinate
Zr(1)	8.011	10.979	4.132
Zr(2)	9.030	6.095	4.079
Zr(3)	6.089	8.089	3.709
Zr(4)	11.021	9.056	3.821
Cl(1)	5.586	11.014	0.091
Cl(2)	11.349	6.074	0.252
Cl(3)	6.351	5.643	7.378
Cl(4)	10.773	11.461	7.625
O(1)	6.776	9.924	2.766
O(2)	9.986	7.548	2.686
O(3)	7.508	7.634	5.224
O(4)	9.644	10.029	5.106
O(5)	7.992	11.843	6.112
O(6)	9.266	5.303	6.207
O(7)	5.432	8.182	1.610
O(8)	11.460	8.966	1.590
O(9)	6.132	12.252	3.491
O(10)	10.948	4.794	3.612
O(11)	4.959	6.154	4.069
O(12)	12.167	11.329	3.644
O(13)	4.184	9.209	4.309
O(14)	13.082	8.359	4.190
O(15)	7.886	4.097	3.663
O(16)	9.291	12.701	3.373
O(17)	6.576	9.649	5.108
O(18)	10.246	7.507	5.133
O(19)	7.648	6.992	2.656
O(20)	9.460	10.131	2.765
O(21)	7.729	11.963	2.193
O(22)	9.233	4.903	2.274
O(23)	5.166	8.020	5.684
O(24)	11.951	9.111	5.846

Table S8. Input parameters, R_w and refined atomic positions for fit of model **T7** to the PDF of $ZrCl_4$ in water. The fit is a one-phase fit of the $[Zr_4(OH)_8(OH_2)_{16}]^{8+}$ -tetramer as refined from the **T5**-model, however, with chloride atoms removed. Hydrogen atoms are not included in the refinement. Atomic positions are not refined for this model.

T6 model			
Parameter	Value		
$B_{iso}(Zr) / \text{\AA}^2$	0.15		
$B_{iso}(O) / \text{\AA}^2$	0.15		
$B_{iso}(Cl) / \text{\AA}^2$	0.15		
Q_{damp}	0.0483		
Q_{broad}	0.0174		
R_w	0.339		
Atom	x-coordinate	y-coordinate	z-coordinate
Zr(1)	8.074	11.004	3.990
Zr(2)	9.126	6.030	3.994
Zr(3)	6.152	8.011	3.764
Zr(4)	11.021	9.056	3.821
O(1)	7.146	9.539	2.641
O(2)	9.962	7.574	2.629
O(3)	7.684	7.222	4.979
O(4)	9.538	9.962	5.092
O(5)	8.017	11.826	5.988
O(6)	9.161	5.081	5.938
O(7)	5.284	8.158	1.564
O(8)	11.826	9.096	1.767
O(9)	6.176	12.438	3.850
O(10)	10.931	4.754	3.852
O(11)	4.873	6.181	3.859
O(12)	12.430	10.934	3.859
O(13)	4.187	9.313	3.969
O(14)	12.890	7.863	3.786
O(15)	7.873	4.258	3.801
O(16)	9.254	12.819	3.742
O(17)	6.732	9.655	5.073
O(18)	10.373	7.456	5.087
O(19)	7.454	6.527	2.824
O(20)	9.654	10.377	2.678
O(21)	7.734	11.802	1.856
O(22)	9.267	5.174	1.875
O(23)	5.104	7.845	5.832
O(24)	11.929	9.266	5.834

Table S9. Input parameters, R_w and refined atomic positions for fit of model **T8** to the PDF of $ZrCl_4$ in water. The fit is a two-phase fit of the $[Zr_4(OH)_8(OH_2)_{16}]^{8+}$ -tetramer as refined from the **T5**-model together with a simulation of the 1st hydration shell of chloride in water. Hydrogen atoms are not included in the refinement. Atomic positions are not refined for this model.

T8 model			
Parameter	Value		
$B_{iso}(Zr) / \text{Å}^2$	0.20		
$B_{iso}(O) / \text{Å}^2$	0.35		
$B_{iso}(Cl) / \text{Å}^2$	0.35		
Q_{damp}	0.0483		
Q_{broad}	0.0174		
R_w	0.204		
Phase 1 (refined fraction: 57.8 %)			
Atom	x-coordinate	y-coordinate	z-coordinate
Zr(1)	8.074	11.004	3.990
Zr(2)	9.126	6.030	3.994
Zr(3)	6.152	8.011	3.764
Zr(4)	11.021	9.056	3.821
Cl(1)	5.169	10.994	0.161
Cl(2)	11.398	6.517	-0.003
Cl(3)	6.665	5.805	7.580
Cl(4)	10.782	11.674	7.483
O(1)	7.146	9.539	2.641
O(2)	9.962	7.574	2.629
O(3)	7.684	7.222	4.979
O(4)	9.538	9.962	5.092
O(5)	8.017	11.826	5.988
O(6)	9.161	5.081	5.938
O(7)	5.284	8.158	1.564
O(8)	11.826	9.096	1.767
O(9)	6.176	12.438	3.850
O(10)	10.931	4.754	3.852
O(11)	4.873	6.181	3.859
O(12)	12.430	10.934	3.859
O(13)	4.187	9.313	3.969
O(14)	12.890	7.863	3.786
O(15)	7.873	4.258	3.801
O(16)	9.254	12.819	3.742
O(17)	6.732	9.655	5.073
O(18)	10.373	7.456	5.087
O(19)	7.454	6.527	2.824
O(20)	9.654	10.377	2.678
O(21)	7.734	11.802	1.856
O(22)	9.267	5.174	1.875
O(23)	5.104	7.845	5.832
O(24)	11.929	9.266	5.834
Phase 2 (refined fraction: 42.2 %)			
Atom	x-coordinate	y-coordinate	z-coordinate
Cl(1)	0	0	0
O(1)	3.169	0	0

2. Variation of concentration on aqueous $ZrCl_4$ solutions

PDFs of aqueous $ZrCl_4$ solutions at various concentrations indicate that the tetramer is present from 0.1-1.5 M, as all the correlations ascribed to the tetramer in the 1 M solution are present in all other solutions (Figure S2). As expected from a lower signal-to-background ratio in the scattering data, decreasing the metal ion concentrations change the PDF peak resolution.

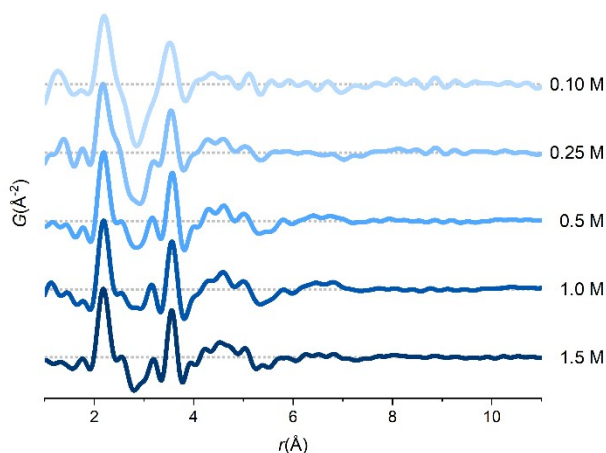


Figure S2. PDFs of aqueous $ZrCl_4$ solutions at various concentrations. The tetramer is present in all solutions. Data collected at P21.1@PETRA-III (0.10 M, 0.25 M, 1.0 M, 1.5 M) and P02.1@PETRA-III (0.5 M).

The upper limit of the studied concentration range was restrained by limited solubility of $ZrCl_4$, as the precursor powder did not fully dissolve in the attempt at making an aqueous 2 M $ZrCl_4$ solution. This explains the turbidity of this solution (Figure S3). The other solutions were completely translucent. No attempts have been made to quantify the exact upper limit of dissolution.

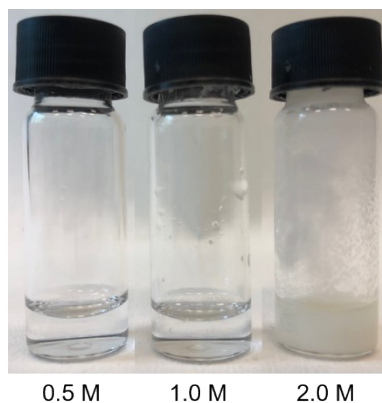


Figure S3. Images of some of the samples used in the concentration series of aqueous $ZrCl_4$ solutions.

Both the raw scattering data and the obtained PDF confirm that long-range order is still present in the sample (Figure S4). Distinct Bragg peaks are present in the scattering data and correlations in the PDF extends to well over 50 Å. In the range of 0-10 Å, the peaks characteristic for the tetramer are all present, indicating that although longer-range order is present, tetramers are an inherent part of the saturated solution.

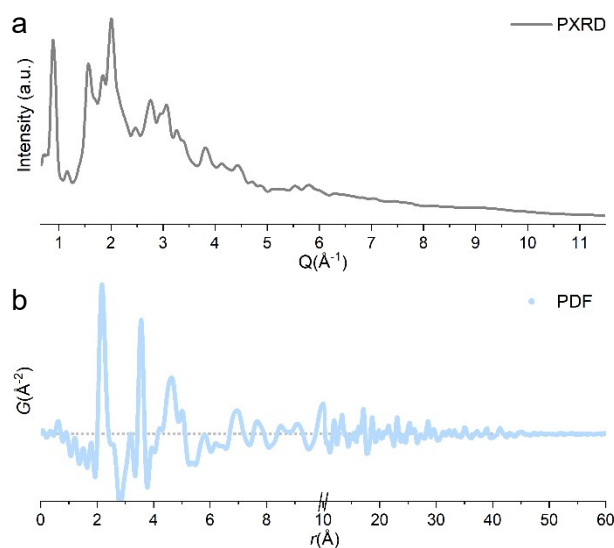


Figure S4. Raw scattering data and PDF of 2 M $ZrCl_4$ sample. Data collected at P02.1@PETRA-III.

3. PDFs of dilute HCl solutions

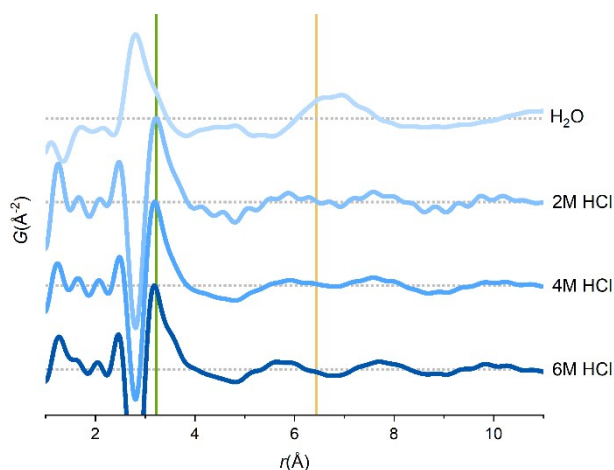


Figure S5. PDFs of dilute HCl solutions at different concentrations and in comparison with water. Green line indicates 1st Cl–O correlation in the hydration shell of chloride in water. Yellow line indicates the position of the peak argued to originate from direct chloride coordination if present within the tetramer. No similar sharp correlations are found in this region for the HCl solutions, thus indicating that the peak observed in the Zr PDFs must originate from a direct interaction of chloride with the tetramer instead. Data collected at P21.1@PETRA-III.

4. Sample images of ZrCl₄ pH series

The pH 0 and 2 samples are completely translucent, whereas for pH 12 and 14, the precipitation of a white gel is observed (Figure S6). For the pH 9 sample, some turbidity is present in the solution, although the PDF mostly resembles the pH 0 and 2 samples.

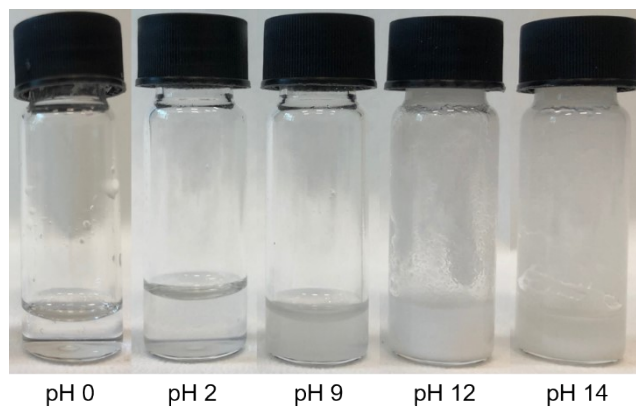


Figure S6. Images of the samples used in the pH series of aqueous ZrCl_4 solutions.

5. Repetitions of aqueous zirconium solutions

The PDFs of the aqueous Zr^{4+} solutions are highly reproducible across repeated measurements on different solutions at different beamlines (Figure S7). Specifically, the small chloride ion feature found only in the aqueous $ZrCl_4$ solutions (insets, Figure S7a) are reproduced across measurements from three beamlines, at two different synchrotron facilities, including the newly commissioned DanMAX beamline at MAX IV. For the $ZrOCl_2$ and $ZrO(NO_3)_2$ solutions, this feature is absent as expected (see discussion in article). These observations and fits to the PDF repetitions (Figure S7b) clearly demonstrate that the peak is not a systematic error or an artefact of the data treatment and that it originates from direct chloride coordination to the tetramer as argued in the article.

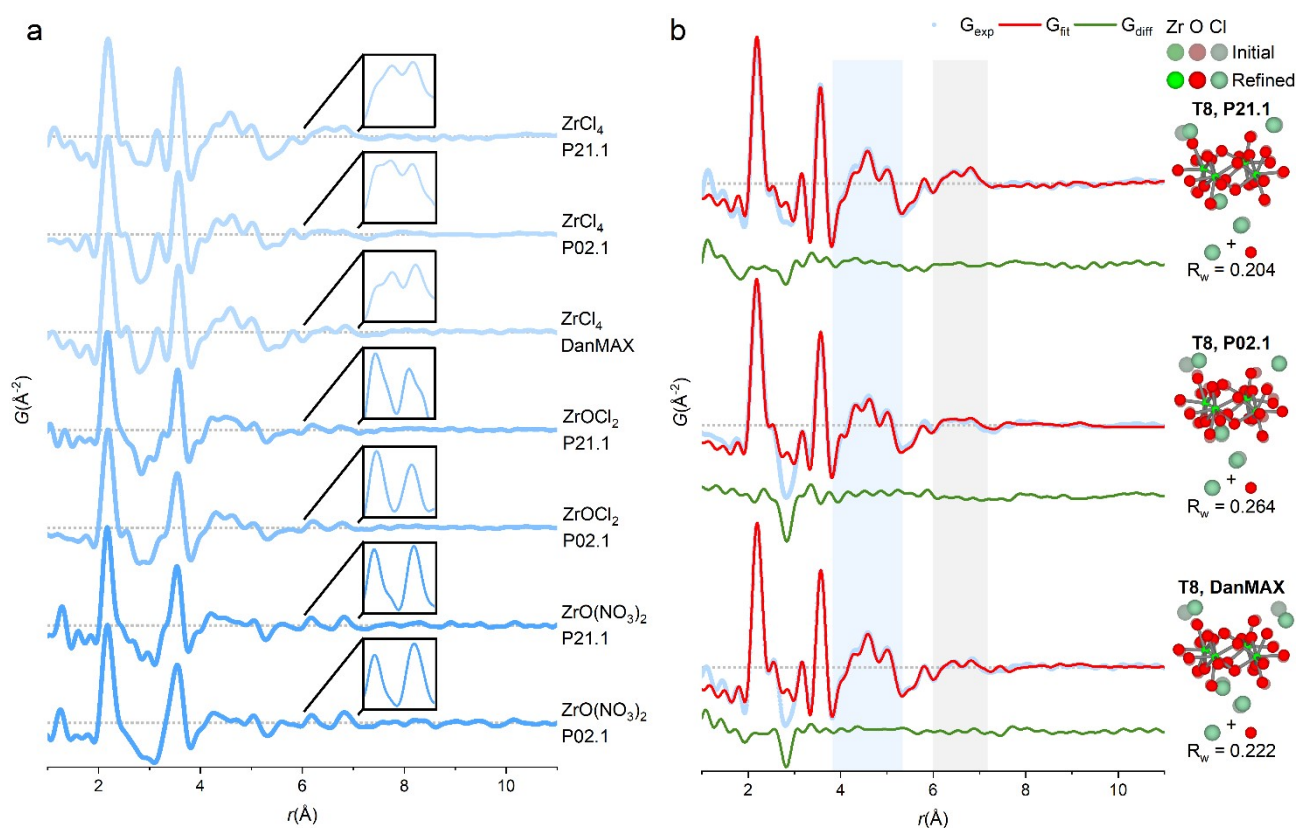


Figure S7. a) PDFs of different zirconium salts dissolved in water used in the article (P21.1@PETRA-III) together with repetitions of the PDFs collected from different solutions at different beamlines (P02.1@PETRA-III and DanMAX@MAX IV). b) PDFs of $ZrCl_4$ in water collected at the different beamlines fitted with tetramer models similar to model **T8**.

6. Modelling of long-period modulation in PDF intensity in methanol and ethanol solutions of ZrCl₄

The PDF of ZrCl₄ in methanol shows a long-period modulation of the intensity, which exceeds the otherwise rigid short-range coherence of the monomers in solution (Figure S8 and S22). The same is observed for the ZrCl₄/ethanol solution (Figure S23). While the *cis*-ZrCl₄O₂-model accounts for all the significant, well-defined peaks in the PDF, the difference curve directly reveals this long-period modulation. Other researchers have previously described similar observations and attributed this to solvent-restructuring effects e.g. on the surface of ZnO nanoparticles² and on bismuth oxido clusters in DMSO solution.³ However, as the amplitudes of the oscillating features observed here are rather small and Q_{\min} dependent (Figure S10-S11), the origin of the features is most likely Q_{\min} dependent Fourier termination ripples.

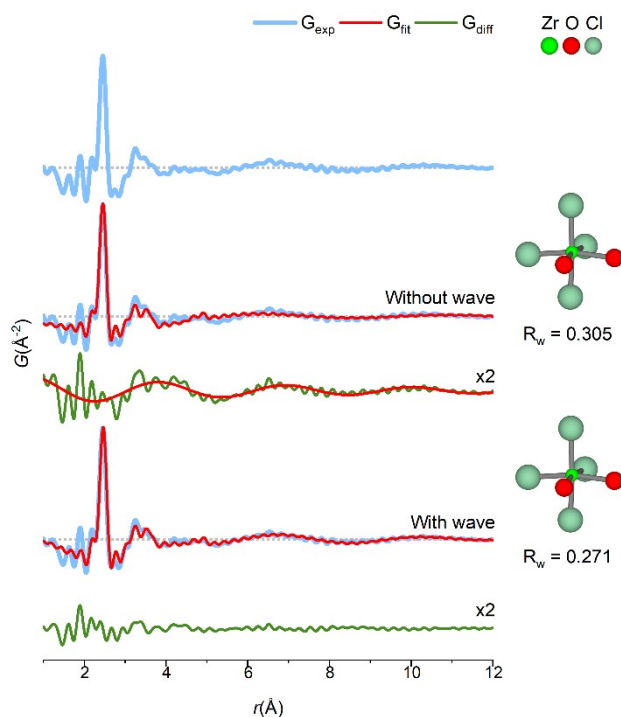


Figure S8. a) Modelling of long-period modulation of intensity in PDF of ZrCl₄ in methanol solution using an exponentially damped sine wave: $y = a \cdot \sin(b \cdot r + c) \cdot \exp(-d \cdot r)$ with the following parameters: $a = 0.1295$, $b = 2.0239$, $c = 0.0801$, $d = 0.1457$. Note: The difference curves have been multiplied by a factor of 2 to highlight the weak long-period intensity modulation. Data collected at P21.1@PETRA-III.

The oscillations in the difference curve can be satisfactorily described by an exponentially damped sinusoidal function. When included in the refinement of the PDF together with the *cis*-ZrCl₄O₂-model, a significantly improved agreement factor (R_w) is achieved (from 0.305 to 0.271), and a completely flat difference curve is obtained. Although we arrive at better description of the PDF in terms of fit and agreement factor, modelling

these features do not change the structural conclusions, i.e. we extract the same information about the Zr^{4+} monomers in the solution regardless. The same modelling approach is used to model the PDFs of $ZrCl_4$ in ethanol, as this PDF show similar long-period modulation (Figure S11 and S23).

7. Tables with refined parameters from fitting PDF of $ZrCl_4$ in non-aqueous solutions

Table S10. Model overview used for fitting the PDF of $ZrCl_4$ in methanol. All models are based on octahedron cutout from crystal structure of $ZrCl_4$ solved by Krebs.⁴ Input parameters can be seen in Table S11-S13.

Model	Comments	Refined	R_w
O1	Octahedron from $ZrCl_4$ crystal structure	÷	0.860
O2	Based on O2 with bond lengths changed to match experimental PDF, but bond angles preserved	÷	0.385
O3 (final)	Based on O3 with two chlorides exchanged with oxygen and bond lengths adjusted to shoulder on main peak in experimental PDF.	÷	0.271

Table S11. Input parameters, R_w , parameters for the exponentially damped sine function: $y = a \cdot \sin(b \cdot r + c) \cdot \exp(-d \cdot r)$ and input atomic positions used for fit of **O1** model (crystal structure (CS) cutout of $ZrCl_6$ octahedron) to the PDF of $ZrCl_4$ in methanol. Atomic positions are not refined for this model.

O1 model (CS $ZrCl_6$) $ZrCl_4$ in methanol			
Parameter	Value		
$B_{iso}(Zr) / \text{Å}^2$	0.15		
$B_{iso}(O) / \text{Å}^2$	0.15		
$B_{iso}(Cl) / \text{Å}^2$	0.15		
Q_{damp}	0.0483		
Q_{broad}	0.0174		
a	0.1295		
b	2.0239		
c	0.0801		
d	0.1457		
R_w	0.860		
Atom	x-coordinate	y-coordinate	z-coordinate
Zr(1)	-0.517	1.215	1.476
Cl(1)	0.632	2.688	2.831
Cl(2)	-1.444	-0.797	0.013
Cl(3)	-2.478	0.797	2.965
Cl(4)	-1.666	2.688	0.121
Cl(5)	0.410	-0.797	2.939
Cl(6)	1.444	0.797	-0.013

Table S12. Input parameters, R_w , parameters for the exponentially damped sine function: $y = a \cdot \sin(b \cdot r + c) \cdot \exp(-d \cdot r)$ and input atomic positions used for fit of **O2** model (adjusted CS cutout of $ZrCl_6$ octahedron) to the PDF of $ZrCl_4$ in methanol. Atomic positions are not refined for this model.

O2 model (adj. CS $ZrCl_6$) $ZrCl_4$ in methanol			
Parameter	Value		
$B_{iso}(Zr) / \text{\AA}^2$	0.15		
$B_{iso}(O) / \text{\AA}^2$	0.15		
$B_{iso}(Cl) / \text{\AA}^2$	0.15		
Q_{damp}	0.0483		
Q_{broad}	0.0174		
a	0.1295		
b	2.0239		
c	0.0801		
d	0.1457		
R_w	0.385		
Atom	x-coordinate	y-coordinate	z-coordinate
Zr(1)	-0.554	0.964	1.517
Cl(1)	0.671	2.534	2.961
Cl(2)	-1.413	-0.901	0.161
Cl(3)	-2.486	0.552	2.983
Cl(4)	-1.779	2.534	0.072
Cl(5)	0.305	-0.901	2.872
Cl(6)	1.377	0.552	0.050

Table S13. Input parameters, R_w , parameters for the exponentially damped sine function: $y = a \cdot \sin(b \cdot r + c) \cdot \exp(-d \cdot r)$ and input atomic positions used for fit of **O3** model (*cis*- $ZrCl_4O_2$) to the PDF of $ZrCl_4$ in methanol. Atomic positions are not refined for this model.

O3 model (<i>cis</i>-$ZrCl_4O_2$) $ZrCl_4$ in methanol			
Parameter	Value		
$B_{iso}(Zr) / \text{\AA}^2$	0.15		
$B_{iso}(O) / \text{\AA}^2$	0.15		
$B_{iso}(Cl) / \text{\AA}^2$	0.15		
Q_{damp}	0.0483		
Q_{broad}	0.0174		
a	0.1295		
b	2.0239		
c	0.0801		
d	0.1457		
R_w	0.271		
Atom	x-coordinate	y-coordinate	z-coordinate
Zr(1)	-0.719	0.929	1.642
Cl(1)	0.506	2.499	3.086
Cl(2)	-1.578	-0.936	0.286
Cl(3)	0.140	-0.936	2.997
Cl(4)	1.212	0.516	0.175
O(1)	-2.486	0.552	2.983
O(2)	-1.839	2.365	0.320

Table S14. Input parameters, R_w , parameters for the exponentially damped sine function: $y = a \cdot \sin(b \cdot r + c) \cdot \exp(-d \cdot r)$ and input atomic positions used for fit of **O3** model (*cis*-ZrCl₄O₂) to the PDF of ZrCl₄ in ethanol. Atomic positions are not refined for this model.

O3 model (<i>cis</i>-ZrCl₄O₂)			
ZrCl₄ in ethanol			
Parameter	Value		
B _{iso} (Zr) / Å ²	0.15		
B _{iso} (O) / Å ²	0.15		
B _{iso} (Cl) / Å ²	0.15		
Q _{damp}	0.0483		
Q _{broad}	0.0174		
a	0.091		
b	1.791		
c	-0.424		
d	0.177		
R _w	0.243		
Atom	x-coordinate	y-coordinate	z-coordinate
Zr(1)	-0.719	0.929	1.642
Cl(1)	0.506	2.499	3.086
Cl(2)	-1.578	-0.936	0.286
Cl(3)	0.140	-0.936	2.997
Cl(4)	1.212	0.516	0.175
O(1)	-2.486	0.552	2.983
O(2)	-1.839	2.365	0.320

Table S15. Input parameters, R_w , parameters for the exponentially damped sine function: $y = a \cdot \sin(b \cdot r + c) \cdot \exp(-d \cdot r)$ and input atomic positions used for fit of *cis*-ZrCl₄N₂ (ideal octahedron) to the PDF of ZrCl₄ in acetonitrile. Atomic positions are not refined for this model.

<i>cis</i> -ZrCl ₄ N ₂ model			
ZrCl ₄ in acetonitrile			
Parameter	Value		
B _{iso} (Zr) / Å ²	0.15		
B _{iso} (N) / Å ²	0.15		
B _{iso} (Cl) / Å ²	0.15		
Q _{damp}	0.0384		
R _w	0.292		
Atom	x-coordinate	y-coordinate	z-coordinate
Zr(1)	4.813	6.465	4.539
Cl(1)	3.793	4.761	3.174
Cl(2)	2.883	6.466	5.982
Cl(3)	3.793	8.170	3.174
Cl(4)	5.834	4.761	5.904
N(1)	6.743	6.466	3.096
N(2)	5.833	8.170	5.904

8. Repetition of methanol and ethanol ZrCl₄ solutions

The PDFs of ZrCl₄ in methanol and ethanol and the structural information they convey are reproducible across repeated measurement at different beamlines using different photon energies and consequently different Q-ranges (Figure S9). The PDFs are not exactly identical, although the data has been collected on identically prepared solutions of ZrCl₄ dissolved in methanol and ethanol. However, the PDFs show all the same features, i.e. structural features limited to a monomeric motif with fits indicating octahedral coordination.

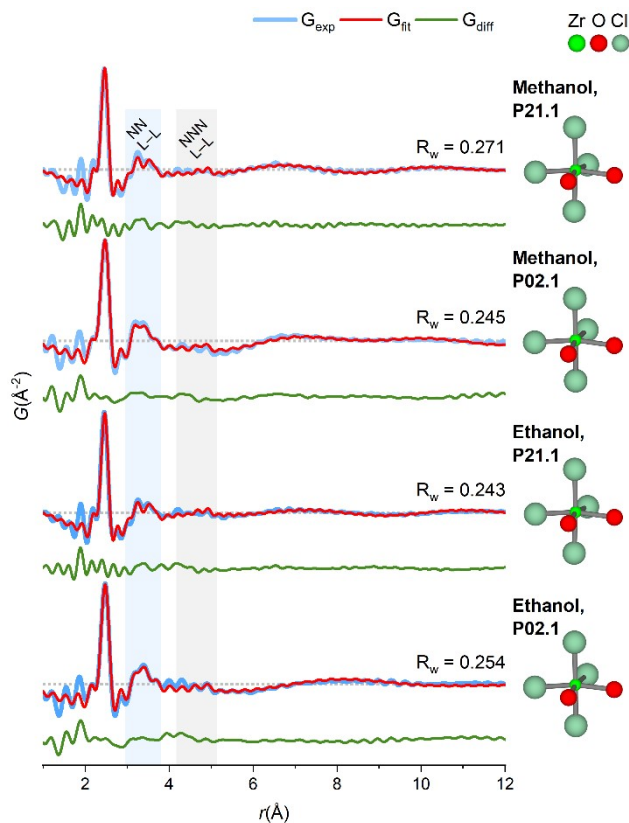


Figure S9. PDFs of $ZrCl_4$ dissolved in methanol and ethanol used in the article (P21.1@PETRA-III) together with repetitions of the PDFs collected from different solutions at a different beamline (P02.1@PETRA-III) all fitted with the same *cis*- $ZrCl_4O_2$ -model used in the article. Small differences in the NN L-L region of the repeated PDFs exist. To relax the models to these differences, atomic positions were allowed to relax with a box restraint of 0.05 Å. In all fits, an exponentially damped sinusoidal function is included in the models to account for long-period modulation of the intensity in the PDFs (see ESI section 6, Figure S8).

Due to setup limitations, the data collected at P21.1@PETRA-III used in the article has an instrumental Q_{\min} of 1.35 \AA^{-1} , while the repetition from P02.1 has an instrumental Q_{\min} of 0.7 \AA^{-1} . From Figure S10a and S11a, it is evident that a Q_{\min} of 1.35 \AA^{-1} cuts off a low angle peak in the raw scattering data, which will consequently not be included in the Fourier transformation to yield the PDF. Notably, however, the Q_{\min} used in the Fourier transformations to yield the PDF has no effect on rigid short-range order of the monomeric motif as demonstrated in Figure S10b and S11b for $ZrCl_4$ /methanol and $ZrCl_4$ /ethanol with P02.1, respectively, where the P02.1 data has been Fourier transformed with varying Q_{\min} . The only differences observed between the PDFs are the slowly oscillating features, which are most likely Q_{\min} dependent Fourier termination ripples, as the oscillation amplitudes and maxima positions varies slightly with Q_{\min} (see slight shift of feature around 6-7

\AA^{-1} , Figure S10b). Consequently, no structural information is lost by using the P21.1 data with the Q_{\min} of 1.35 \AA^{-1} .

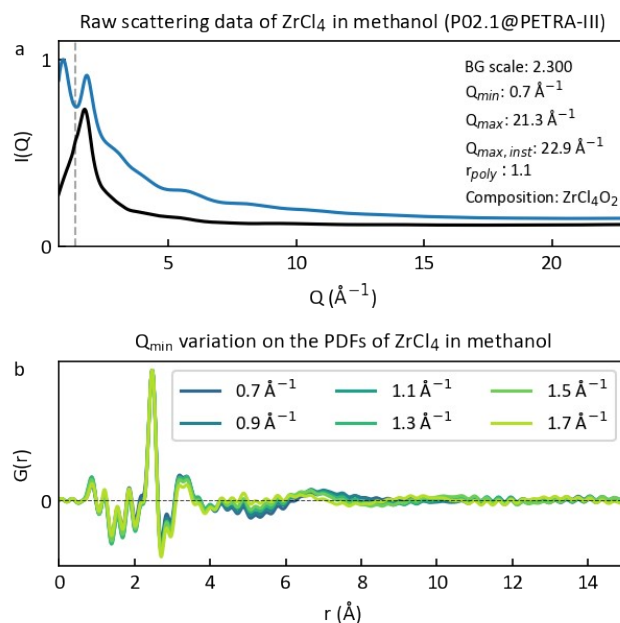


Figure S10. a) Raw scattering data of ZrCl_4 dissolved in methanol together with methanol+kapton background and b) the consequence of varying Q_{\min} on the PDFs. Data collected at P02.1@PETRA-III. Vertical dashed line in a) marks the Q_{\min} used to Fourier transform the P21.1@PETRA-III data used in the article.

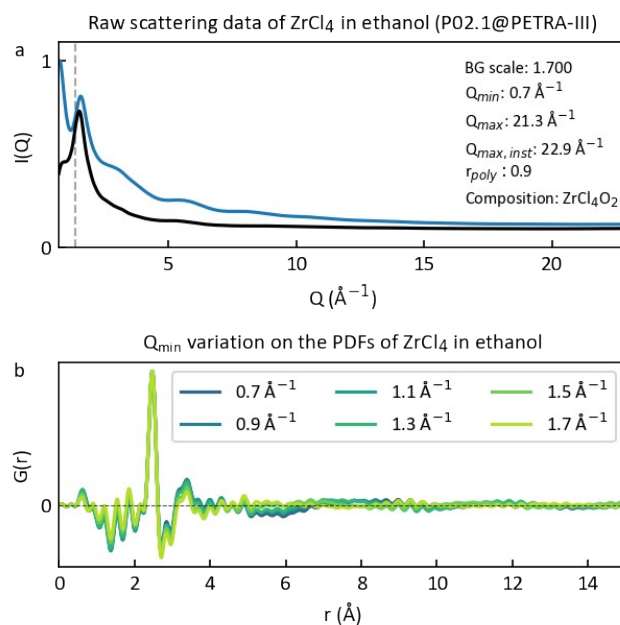


Figure S11. a) Raw scattering data of ZrCl_4 dissolved in ethanol together with ethanol background and b) the consequence of varying Q_{\min} on the PDFs. Data collected at P02.1@PETRA-III. Vertical dashed line in a) marks the Q_{\min} used to Fourier transform the P21.1@PETRA-III data used in the article.

9. Experimental

9.1 Solution preparation

Anhydrous ZrCl_4 (Sigma Aldrich, 99.99%), $\text{ZrOCl}_2 \cdot 8\text{H}_2\text{O}$ (Sigma Aldrich, 99.5%) and $\text{ZrO}(\text{NO}_3)_2 \cdot x\text{H}_2\text{O}$ (Sigma Aldrich, 99%) were used without further purification. The zirconium salts were dissolved in either deionized water, absolute ethanol, methanol or anhydrous acetonitrile to a total metal concentration of 1 M. Since the exact degree of hydration is unknown for $\text{ZrO}(\text{NO}_3)_2 \cdot x\text{H}_2\text{O}$, only an approximate 1 M concentration was obtained. Upon dissolution, translucent solutions were obtained with no sign of gelation. For all 1 M aqueous solutions, the pH was 0. A series of ZrCl_4 solutions with concentrations ranging from 0.1-1.5 M was made to see the effect of dilution on the solution structures.

A pH series was made by dissolving ZrCl_4 in diluted NaOH solutions with concentrations of 1, 2, 3 and 6 M such that pH values of 2, 9, 12 and 14, respectively, were obtained. The total zirconium concentration was maintained at 1 M. For pH 12 and 14, the alkalinity of the solutions resulted in gelation (Figure S6).

Another series was made by dissolving $\text{ZrOCl}_2 \cdot 8\text{H}_2\text{O}$ in HCl solutions with concentration of 2, 4 and 6 M while maintaining the total zirconium concentration at 1 M.

All samples were prepared immediately prior to measurement.

9.2 Total scattering experiments

Total scattering (TS) experiments were conducted at the P02.1 and P21.1 beamlines at PETRA-III (DESY, Hamburg, Germany) using photon energies of ~ 60 keV ($\lambda = 0.2072$ Å) and ~ 100 keV ($\lambda = 0.1204$ Å), respectively, as well as at the DanMAX beamline at MAX IV (Lund, Sweden) using photon energy of ~ 35 keV ($\lambda = 0.3553$ Å). Both PETRA-III beamlines feature 2D Perkin Elmer XRD 1621 area detectors for data acquisition, whereas DanMAX feature a Dectris PILATUS3 X CdTe 2M area detector. At P02.1, the sample-

to-detector distance was ~ 20 cm allowing for an instrumental Q_{\max} of 22.9 \AA^{-1} , whereas the distance was ~ 30 cm at P21.1 giving a Q_{\max} of 28.8 \AA^{-1} and it was ~ 9.3 cm at DanMAX giving a Q_{\max} of 20.5 \AA^{-1} .

The solutions were loaded into 1.45 mm and 1.00 mm Kapton capillary tubes sealed with epoxy at PETRA-III and MAX-IV, respectively. Data acquisition was performed at ambient conditions with an acquisition time of 5-10 min per experiment. Background measurements of the solvent loaded into Kapton capillaries were performed to account for air, capillary and solvent scattering.

9.3 Data treatment

The 2D detector images were integrated using the Dioptas 0.5.2 software⁵ and calibrated using measurements of a LaB₆ NIST SRM 660b line standard. To obtain the real-space PDFs, the data were subsequently treated using the xPDFsuite software⁶ which utilizes the *ad-hoc* correction procedures of PDFgetX3⁷ to perform the Fourier transform of the reduced scattering data. From the raw scattering data of the Zr⁴⁺ solutions, a background measurement of the appropriate solvent is subtracted to isolate scattering contribution stemming from the perturbation of the solvent by dissolving the Zr⁴⁺ species in the solvent.

In Figure S12-S39, $I(Q)$ with scaled background measurement used for background subtraction, $F(Q)$, $S(Q)$ and $G(r)$ as well as the applied Q -range, r_{poly} and composition used in generating the PDF is given for all PDFs used in the article and SI in the order of appearance.

Modelling of the PDFs were performed using DiffPy CMI⁸ by fitting and refining input clusters to the data. Refinement of atomic positions was allowed within a small box around the input positions for certain models.

9.4 PDF generation

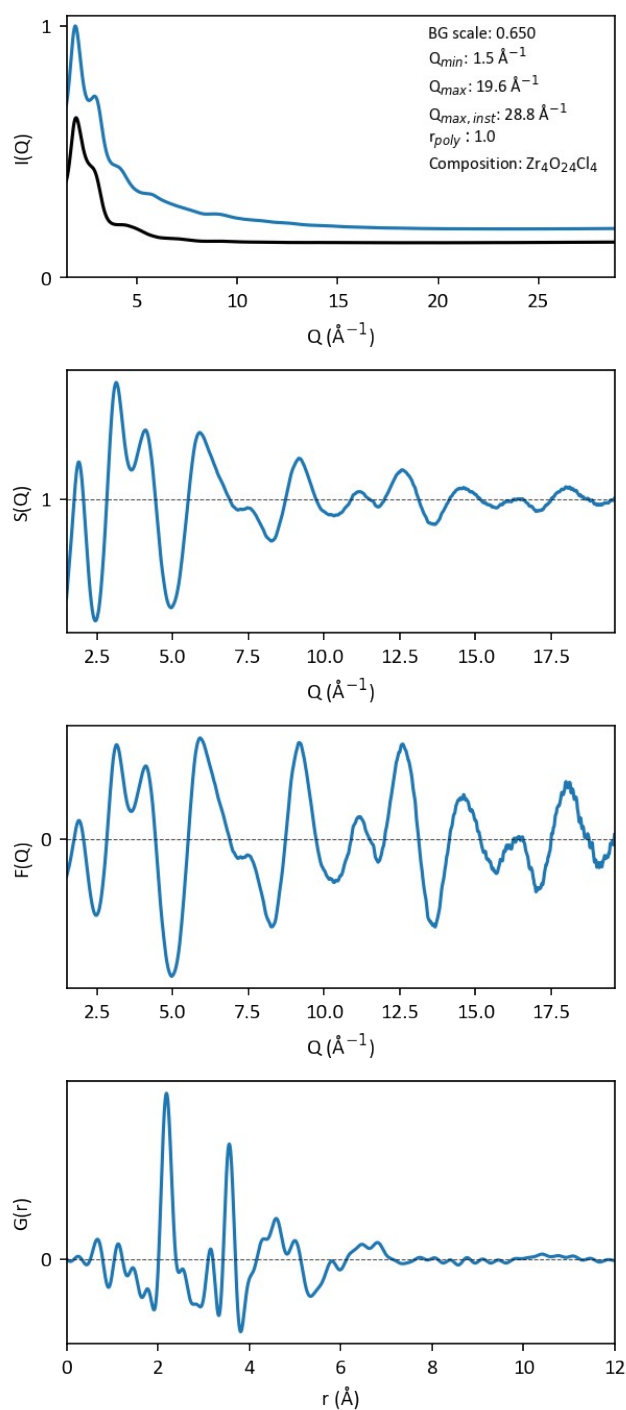


Figure S12. PDF generation of ZrCl_4 in H_2O (1 M) with data collected at beamline P21.1@PETRA-III. a) $I(Q)$ and scaled water background used for background subtraction, b) $S(Q)$, c) $F(Q)$ and d) $G(r)$. The parameters used to generate the PDF in xPDFSuite is given in the figure.

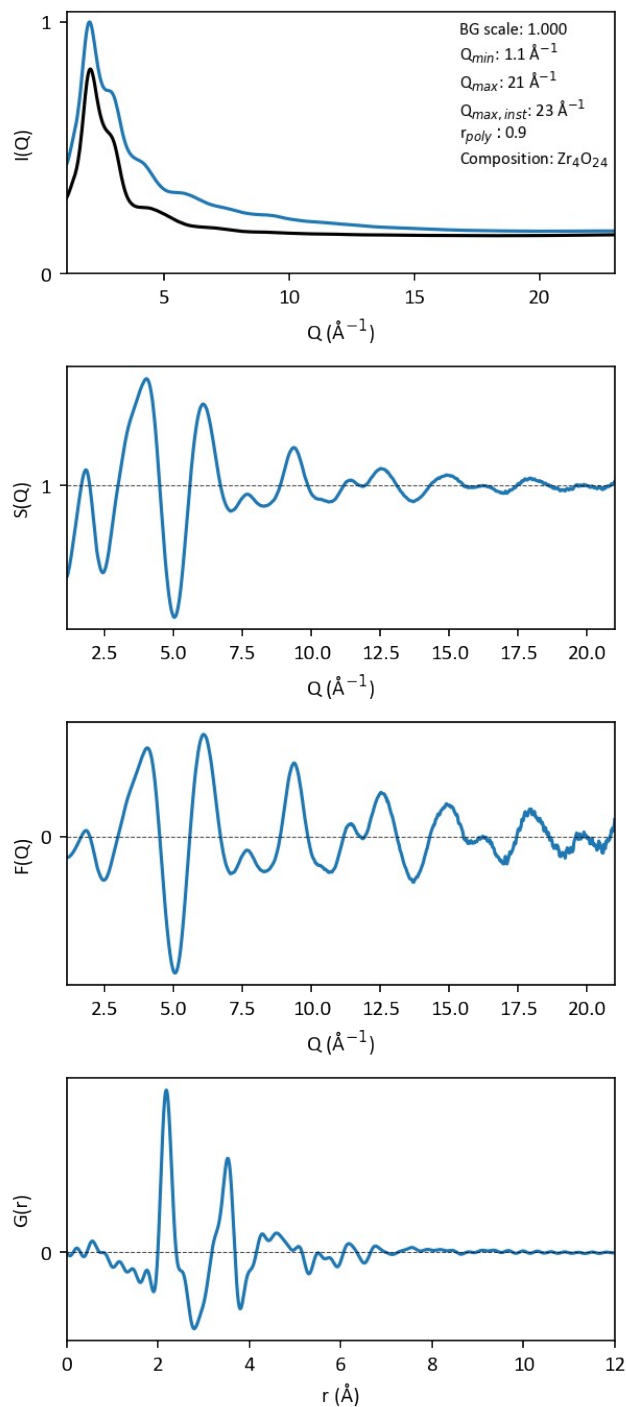


Figure S13. PDF generation of $ZrCl_4$ in aqueous NaOH (1 M, pH 2) with data collected at P02.1@PETRA-III. a) $I(Q)$ and scaled 1 M NaOH background used for background subtraction, b) $S(Q)$, c) $F(Q)$ and d) $G(r)$. The parameters used to generate the PDF in xPDFSuite is given in the figure.

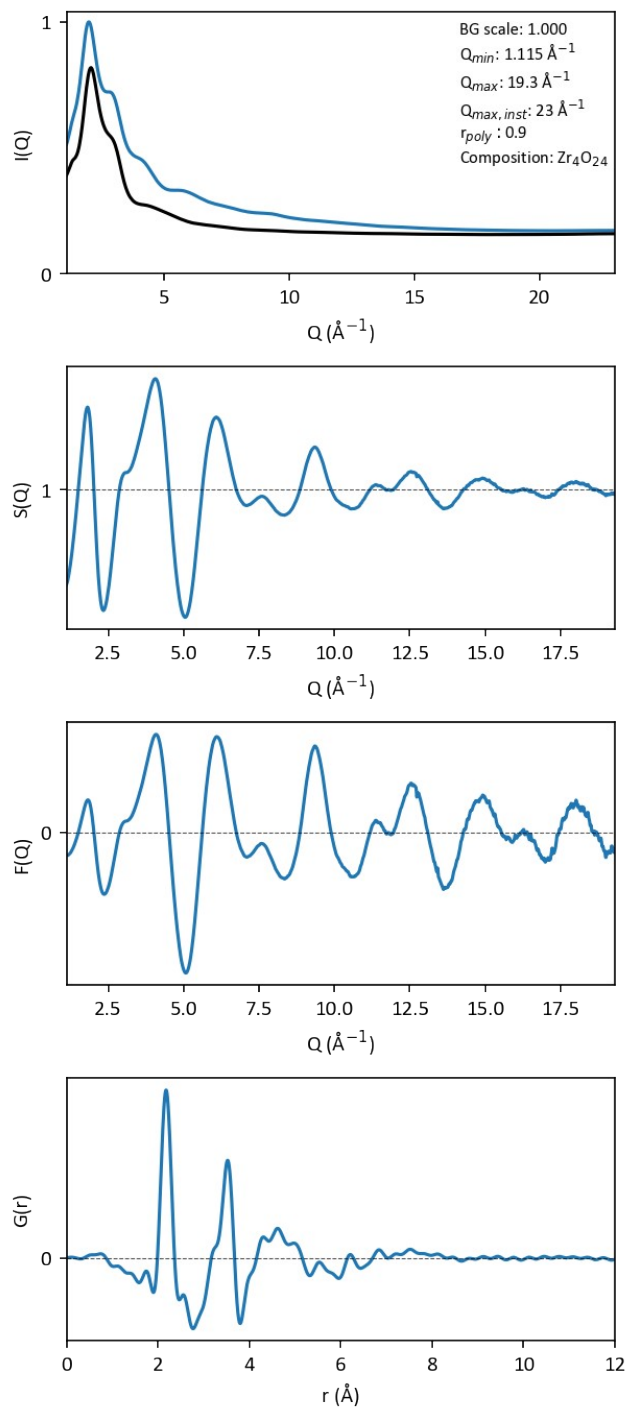


Figure S14. PDF generation of $ZrCl_4$ in aqueous NaOH (2 M, pH 9) with data collected at P02.1@PETRA-III. a) $I(Q)$ and scaled 2 M NaOH background used for background subtraction, b) $S(Q)$, c) $F(Q)$ and d) $G(r)$. The parameters used to generate the PDF in xPDFSuite is given in the figure.

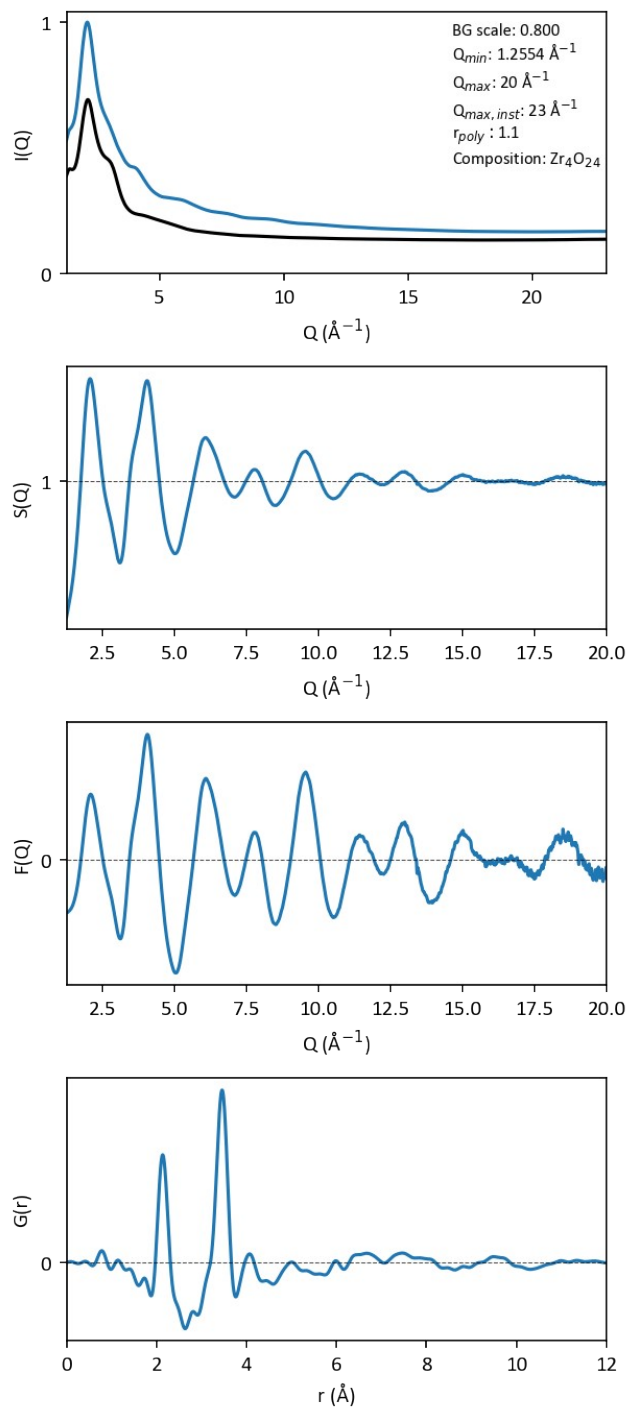


Figure S15. PDF generation of $ZrCl_4$ in aqueous NaOH (3 M, pH 12) with data collected at P02.1@PETRA-III. a) $I(Q)$ and scaled 3 M NaOH background used for background subtraction, b) $S(Q)$, c) $F(Q)$ and d) $G(r)$. The parameters used to generate the PDF in xPDFSuite is given in the figure.

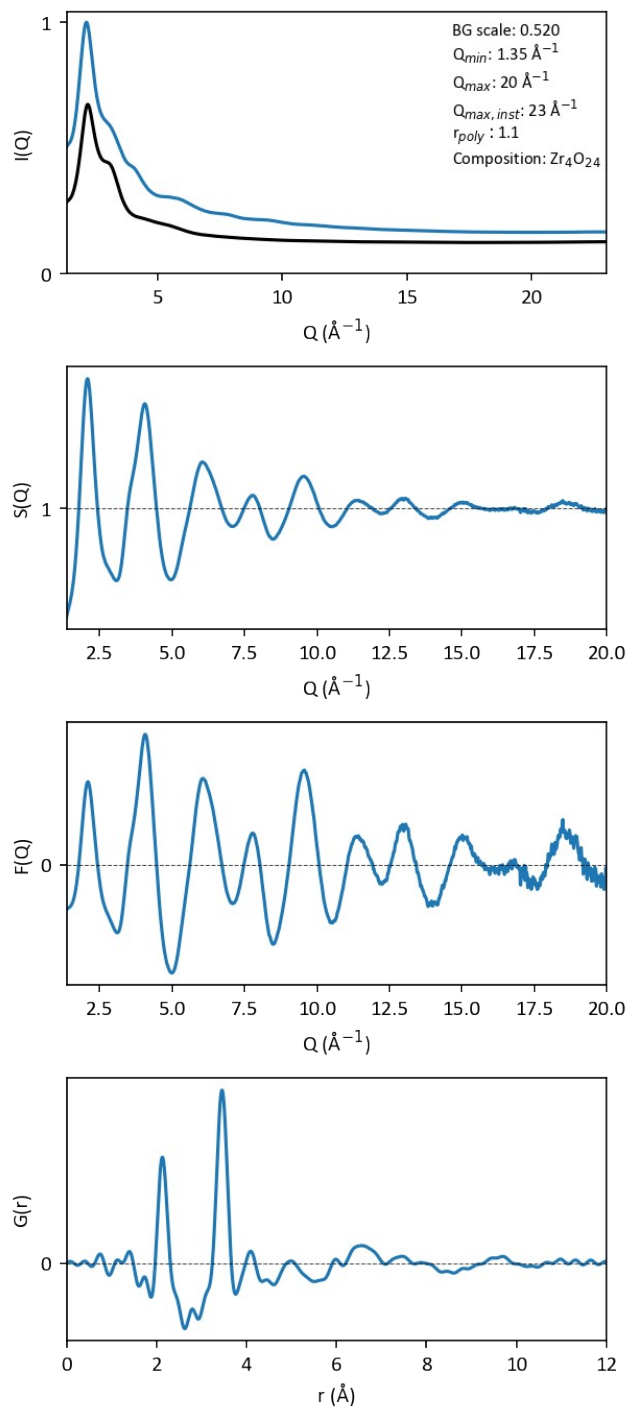


Figure S16. PDF generation of $ZrCl_4$ in aqueous NaOH (6 M, pH 14) with data collected at P02.1@PETRA-III. a) $I(Q)$ and scaled 6 M NaOH background used for background subtraction, b) $S(Q)$, c) $F(Q)$ and d) $G(r)$. The parameters used to generate the PDF in xPDFSuite is given in the figure.

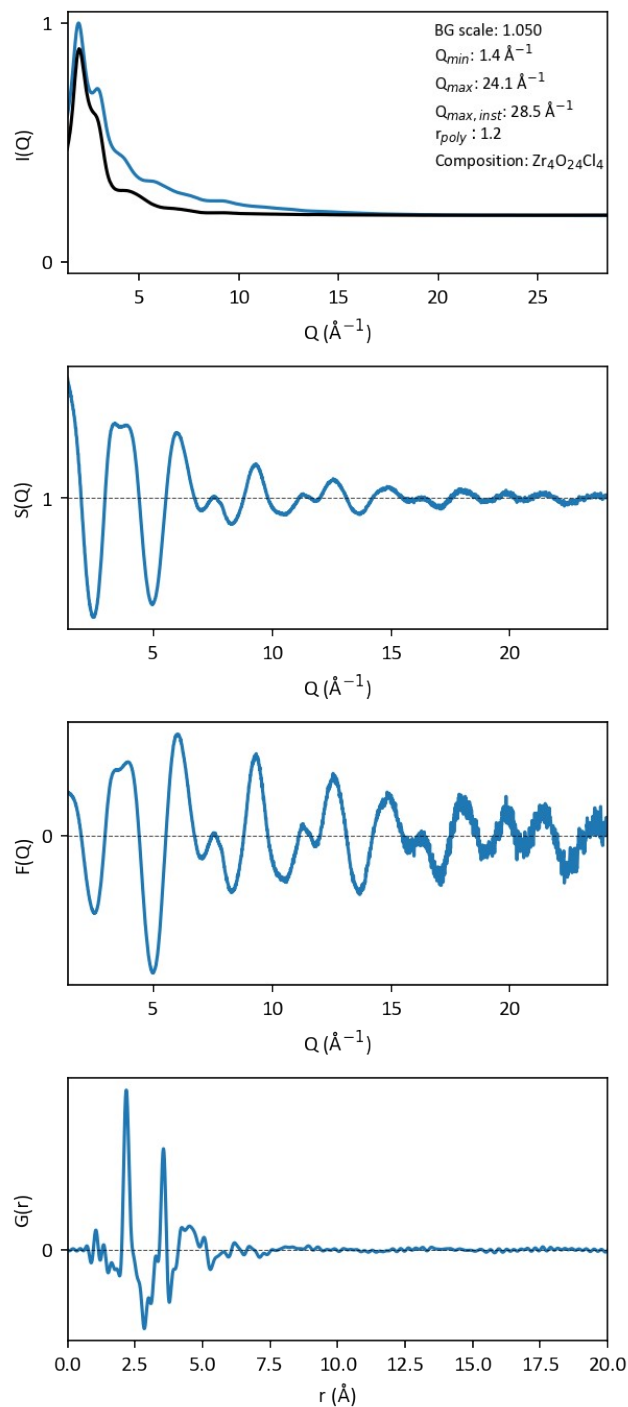


Figure S17. PDF generation of $ZrOCl_2$ in H_2O (1 M) with data collected at P21.1@PETRA-III. a) $I(Q)$ and scaled water background used for background subtraction, b) $S(Q)$, c) $F(Q)$ and d) $G(r)$. The parameters used to generate the PDF in xPDFSuite is given in the figure.

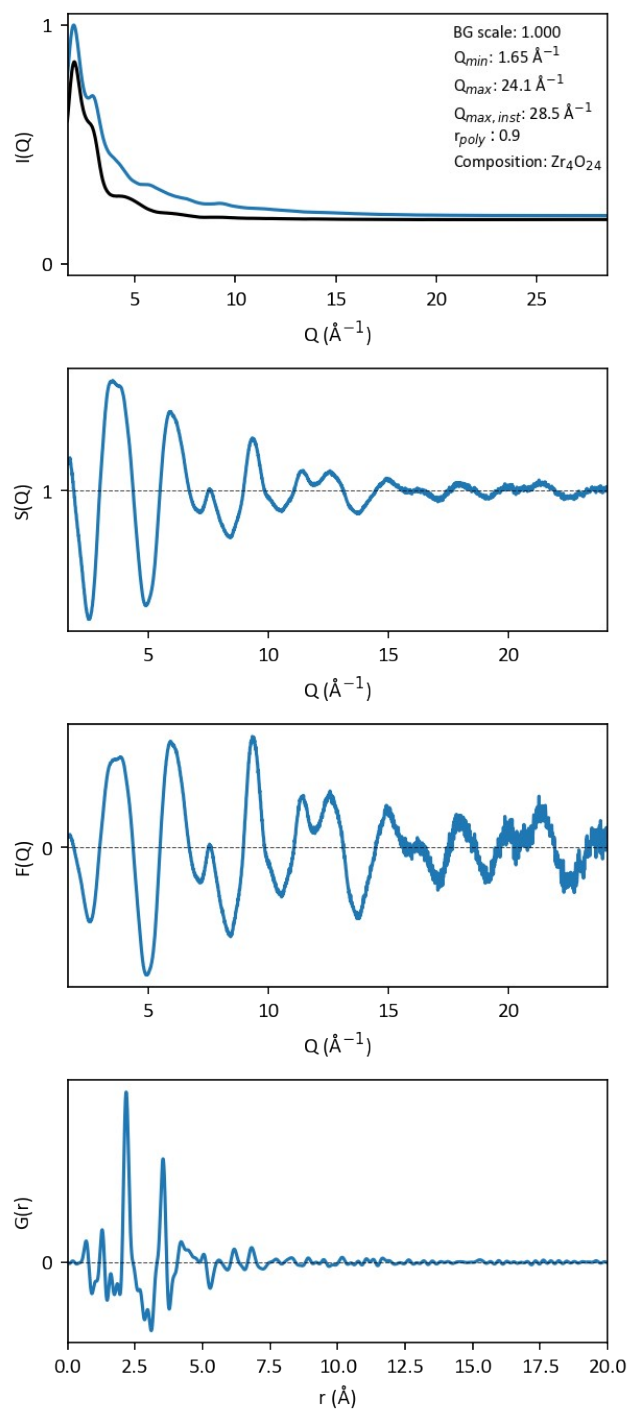


Figure S18. PDF generation of $\text{ZrO}(\text{NO}_3)_2$ in H_2O (1 M) with data collected at P21.1@PETRA-III. a) $I(Q)$ and scaled water background used for background subtraction, b) $S(Q)$, c) $F(Q)$ and d) $G(r)$. The parameters used to generate the PDF in xPDFSuite is given in the figure.

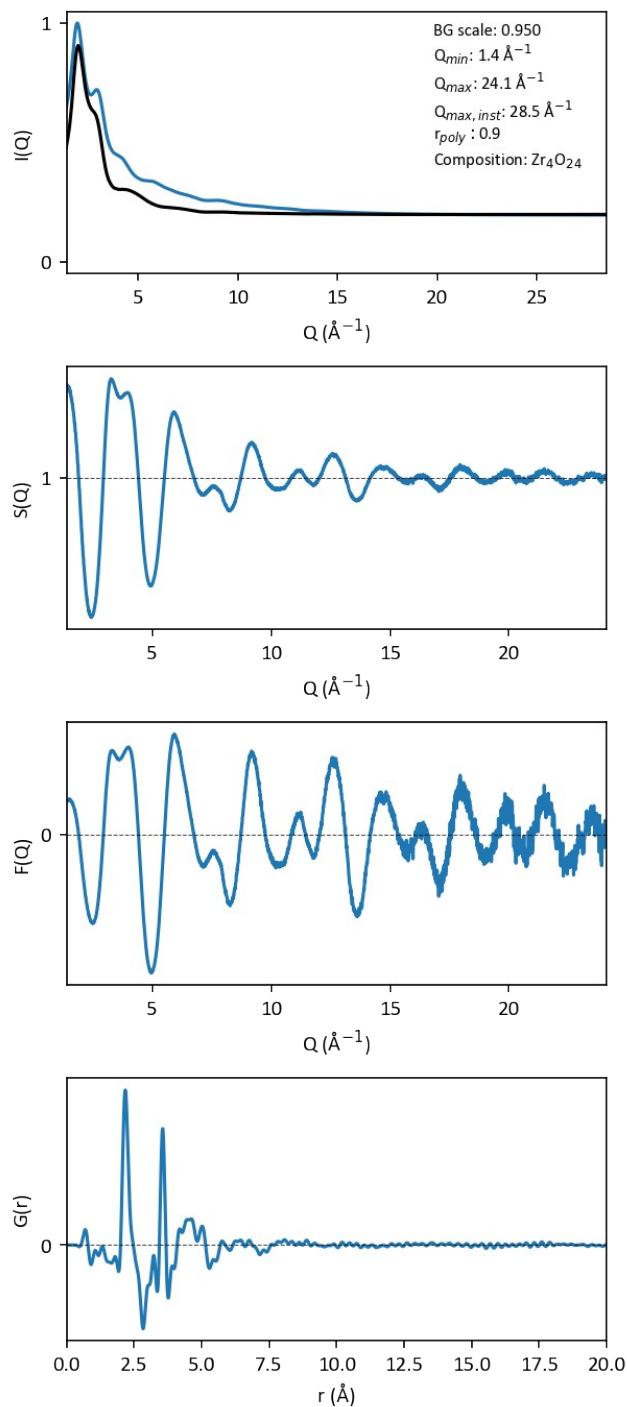


Figure S19. PDF generation of $ZrOCl_2$ in aqueous HCl (2 M, $[Cl^-]/[Zr^{4+}] = 4$) with data collected at P21.1@PETRA-III. a) $I(Q)$ and scaled water background used for background subtraction, b) $S(Q)$, c) $F(Q)$ and d) $G(r)$. The parameters used to generate the PDF in xPDFSuite is given in the figure.

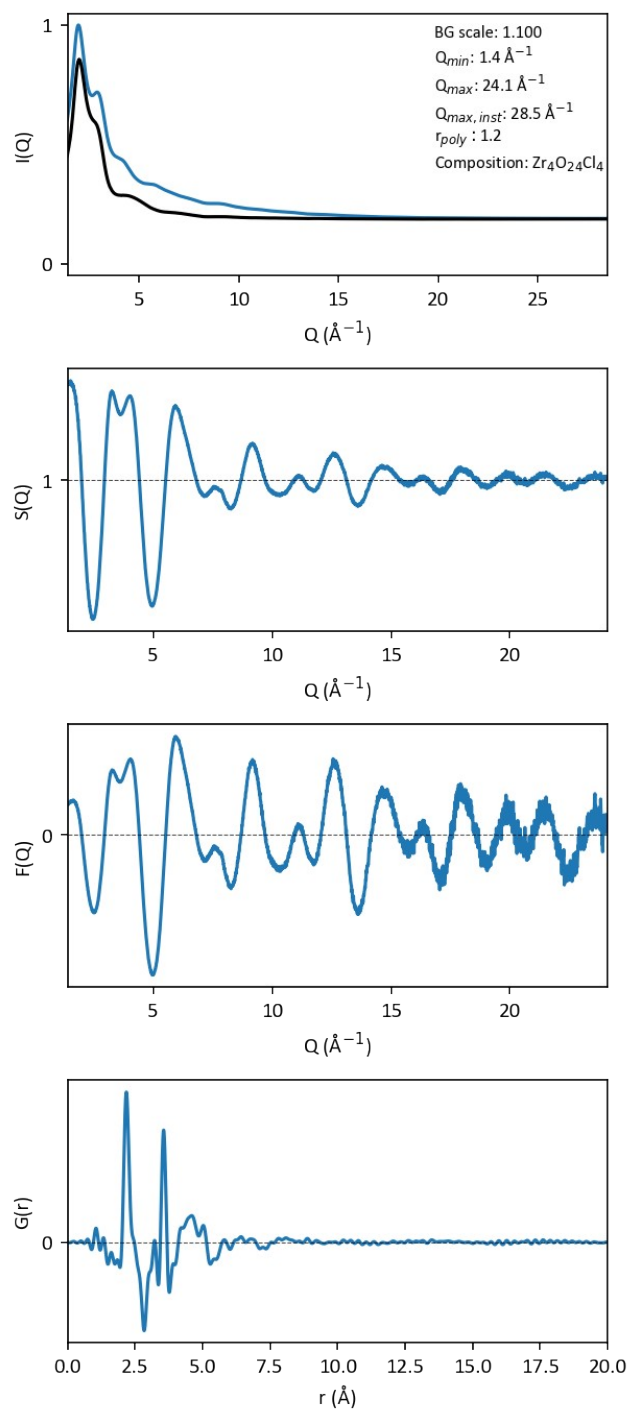


Figure S20. PDF generation of $ZrOCl_2$ in aqueous HCl (4 M, $[Cl^-]/[Zr^{4+}] = 6$) with data collected at P21.1@PETRA-III. a) $I(Q)$ and scaled water background used for background subtraction, b) $S(Q)$, c) $F(Q)$ and d) $G(r)$. The parameters used to generate the PDF in xPDFSuite is given in the figure.

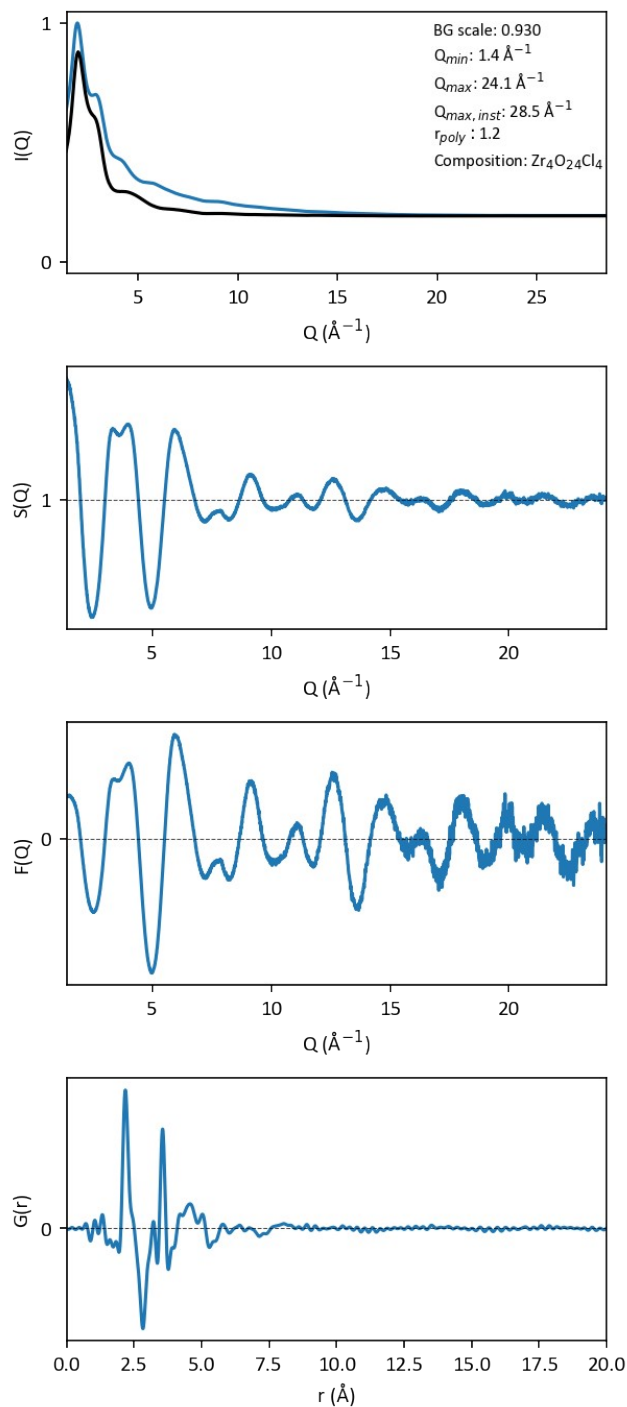


Figure S21. PDF generation of $ZrOCl_2$ in aqueous HCl (6 M, $[Cl^-]/[Zr^{4+}] = 8$) with data collected at P21.1@PETRA-III. a) $I(Q)$ and scaled water background used for background subtraction, b) $S(Q)$, c) $F(Q)$ and d) $G(r)$. The parameters used to generate the PDF in xPDFSuite is given in the figure.

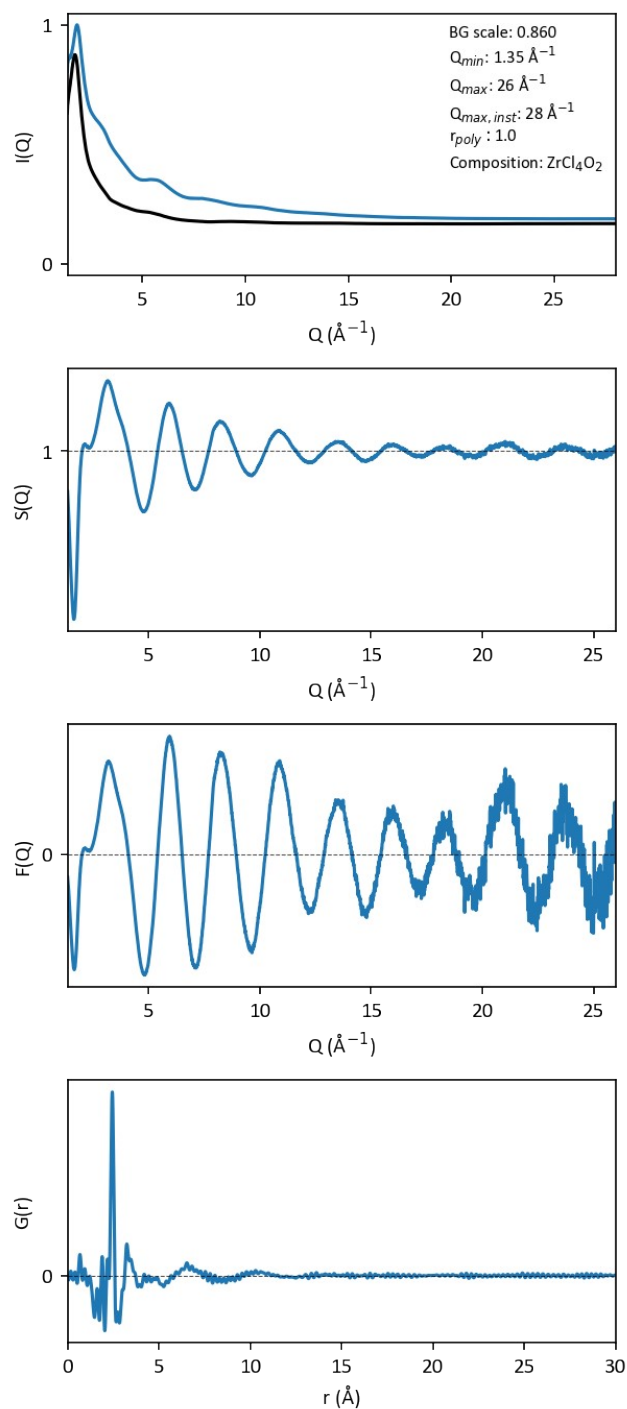


Figure S22. PDF generation of ZrCl_4 in methanol (1 M) with data collected at P21.1@PETRA-III. a) $I(Q)$ and scaled methanol background used for background subtraction, b) $S(Q)$, c) $F(Q)$ and d) $G(r)$. The parameters used to generate the PDF in xPDFSuite is given in the figure.

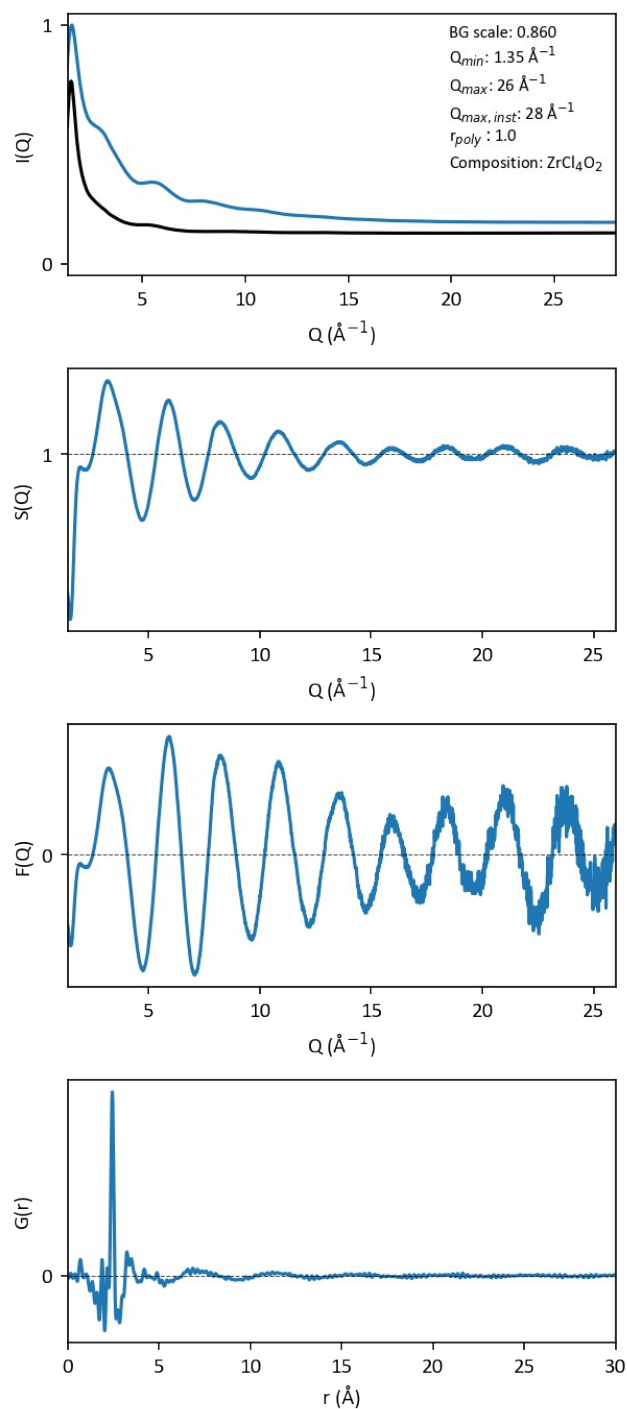


Figure S23. PDF generation of ZrCl_4 in ethanol (1 M) with data collected at P21.1@PETRA-III. a) $I(Q)$ and scaled ethanol background used for background subtraction, b) $S(Q)$, c) $F(Q)$ and d) $G(r)$. The parameters used to generate the PDF in xPDFSuite is given in the figure.

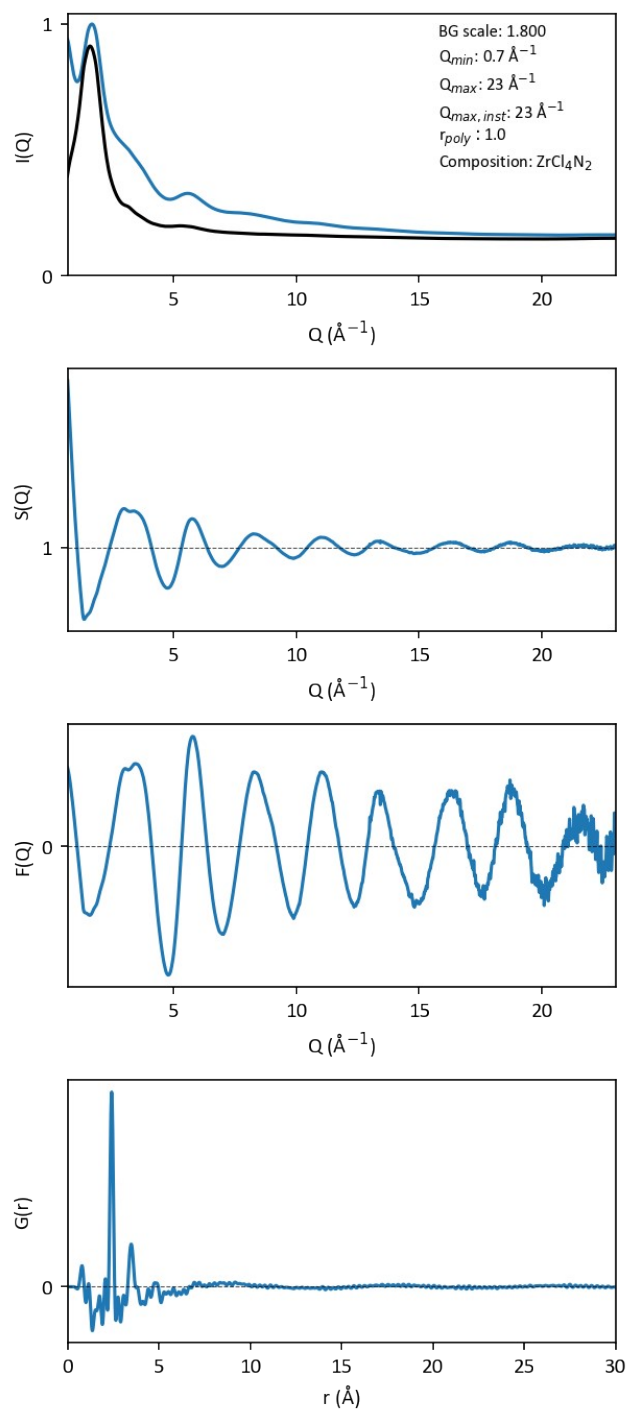


Figure S24. PDF generation of ZrCl_4 in acetonitrile (1 M) with data collected at P02.1@PETRA-III. a) $I(Q)$ and scaled acetonitrile background used for background subtraction, b) $S(Q)$, c) $F(Q)$ and d) $G(r)$. The parameters used to generate the PDF in xPDFSuite is given in the figure.

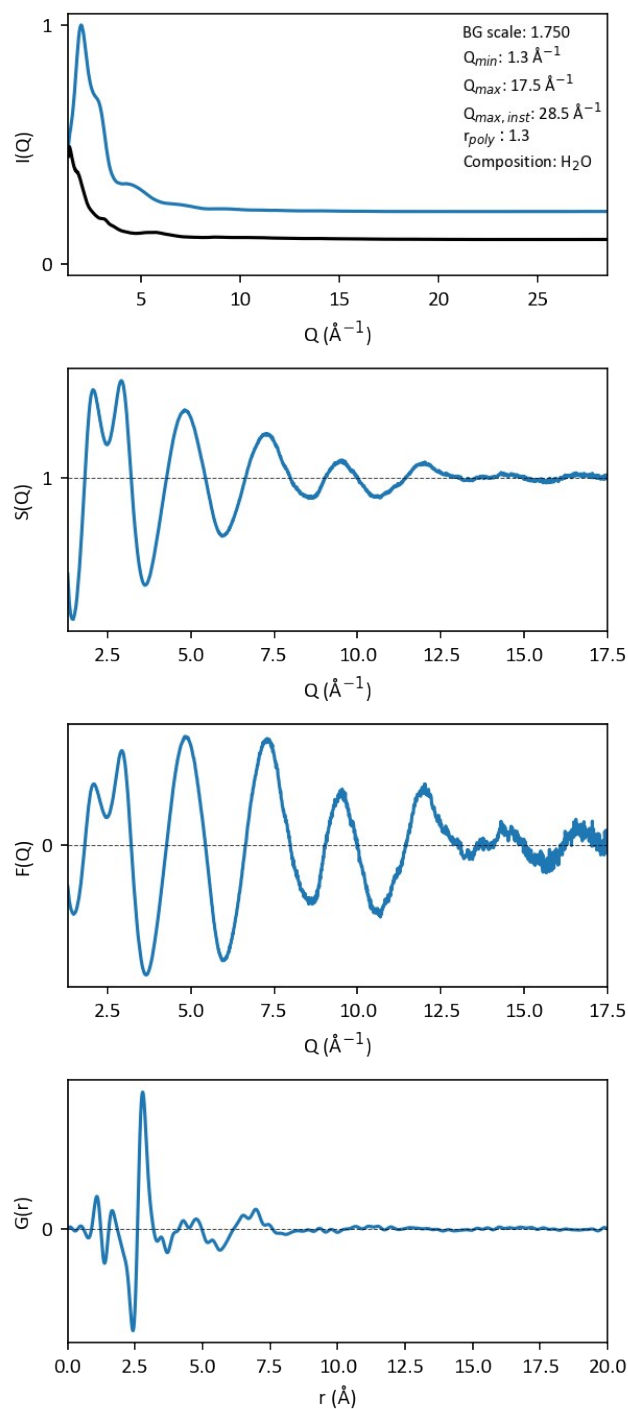


Figure S25. PDF generation of H₂O with data collected at P21.1@PETRA-III. a) $I(Q)$ and scaled Kapton background used for background subtraction, b) $S(Q)$, c) $F(Q)$ and d) $G(r)$. The parameters used to generate the PDF in xPDFSuite is given in the figure.

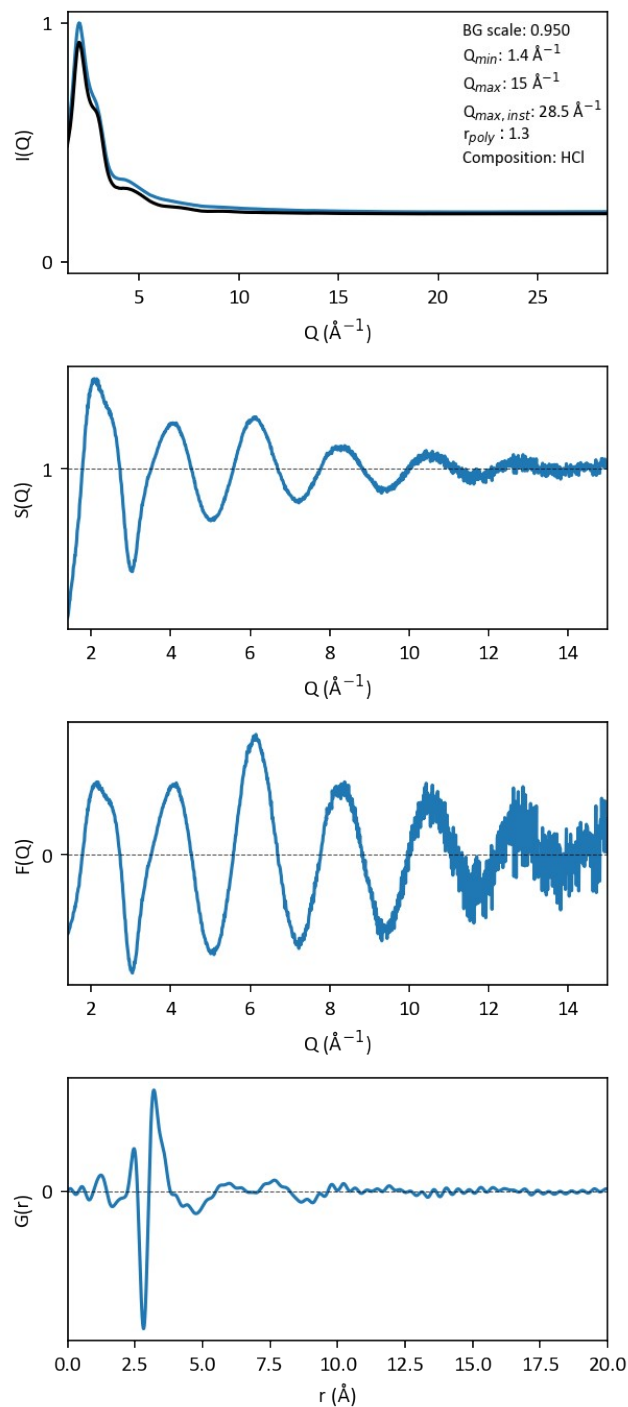


Figure S26. PDF generation of HCl (2 M) with data collected at P21.1@PETRA-III. a) $I(Q)$ and scaled water background used for background subtraction, b) $S(Q)$, c) $F(Q)$ and d) $G(r)$. The parameters used to generate the PDF in xPDFSuite is given in the figure.

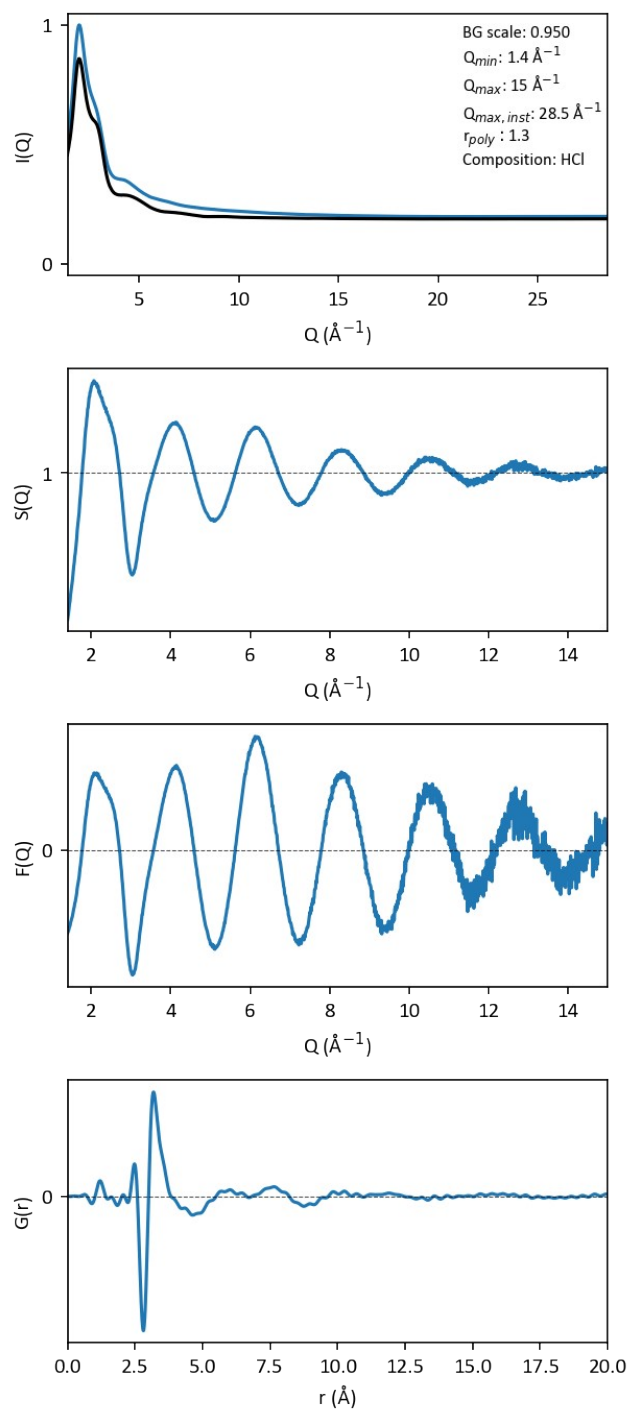


Figure S27. PDF generation of HCl (4 M) with data collected at P21.1@PETRA-III. a) $I(Q)$ and scaled water background used for background subtraction, b) $S(Q)$, c) $F(Q)$ and d) $G(r)$. The parameters used to generate the PDF in xPDFSuite is given in the figure.

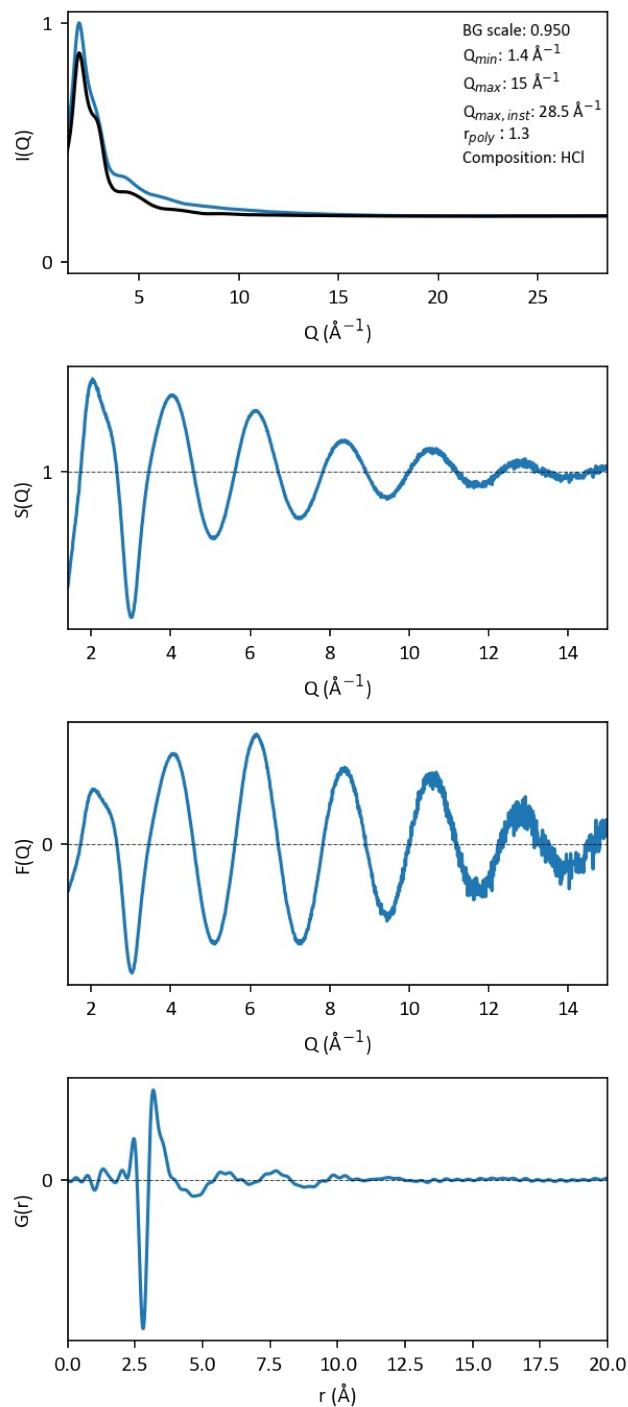


Figure S28. PDF generation of HCl (6 M) with data collected at P21.1@PETRA-III. a) $I(Q)$ and scaled water background used for background subtraction, b) $S(Q)$, c) $F(Q)$ and d) $G(r)$. The parameters used to generate the PDF in xPDFSuite is given in the figure.

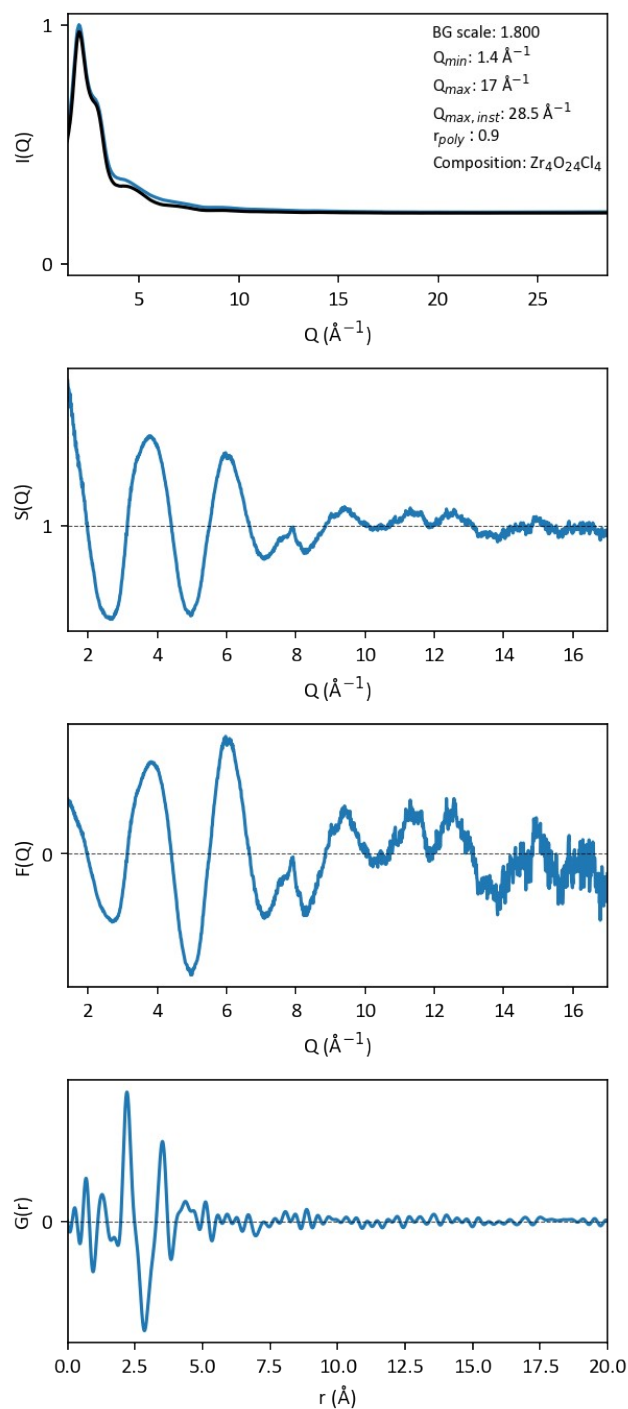


Figure S29. PDF generation of ZrCl_4 in H_2O (0.1 M) with data collected at P21.1@PETRA-III. a) $I(Q)$ and scaled water background used for background subtraction, b) $S(Q)$, c) $F(Q)$ and d) $G(r)$. The parameters used to generate the PDF in xPDFSuite is given in the figure.

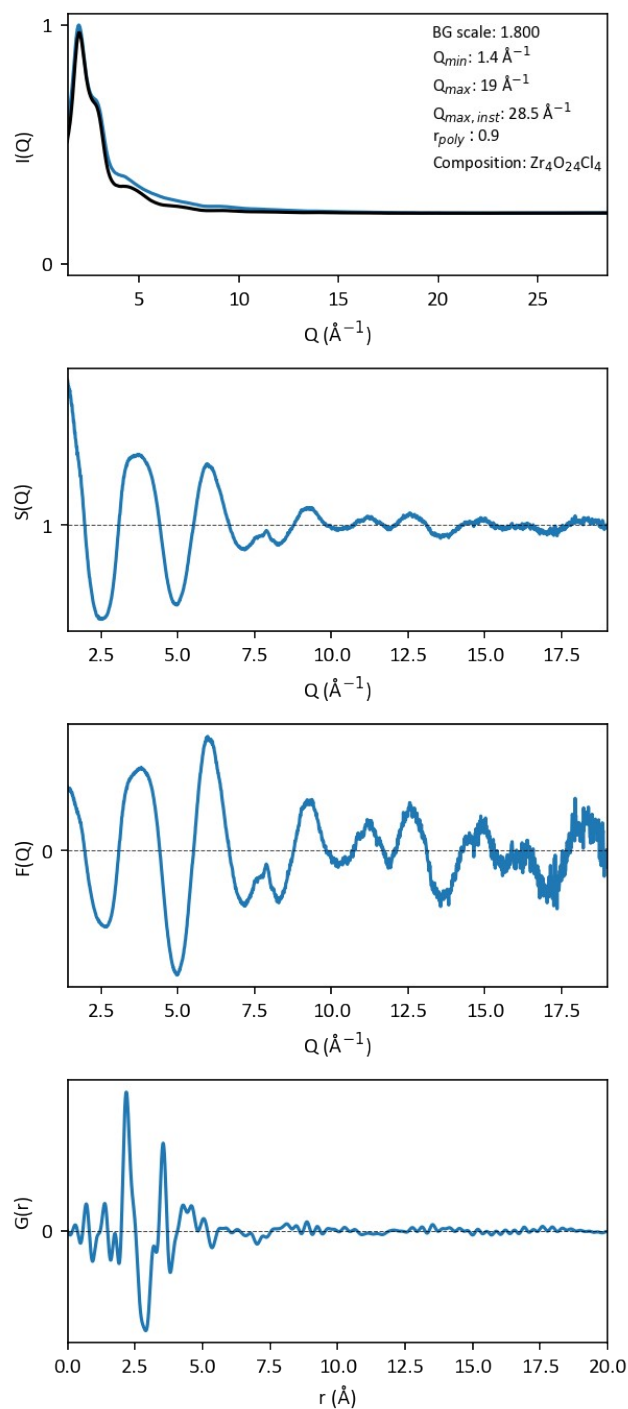


Figure S30. PDF generation of $ZrCl_4$ in H_2O (0.25 M) with data collected at P21.1@PETRA-III. a) $I(Q)$ and scaled water background used for background subtraction, b) $S(Q)$, c) $F(Q)$ and d) $G(r)$. The parameters used to generate the PDF in xPDFSuite is given in the figure.

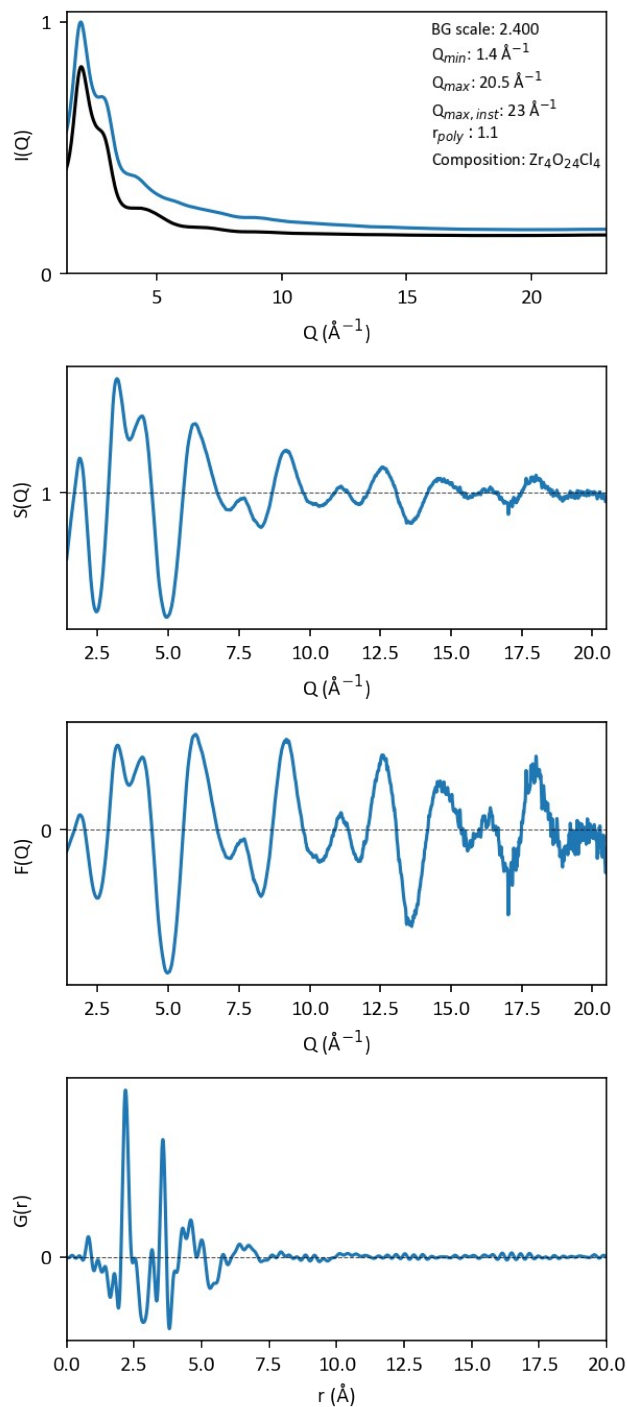


Figure S31. PDF generation of $ZrCl_4$ in H_2O (0.5 M) with data collected at P02.1@PETRA-III. a) $I(Q)$ and scaled water background used for background subtraction, b) $S(Q)$, c) $F(Q)$ and d) $G(r)$. The parameters used to generate the PDF in xPDFSuite is given in the figure.

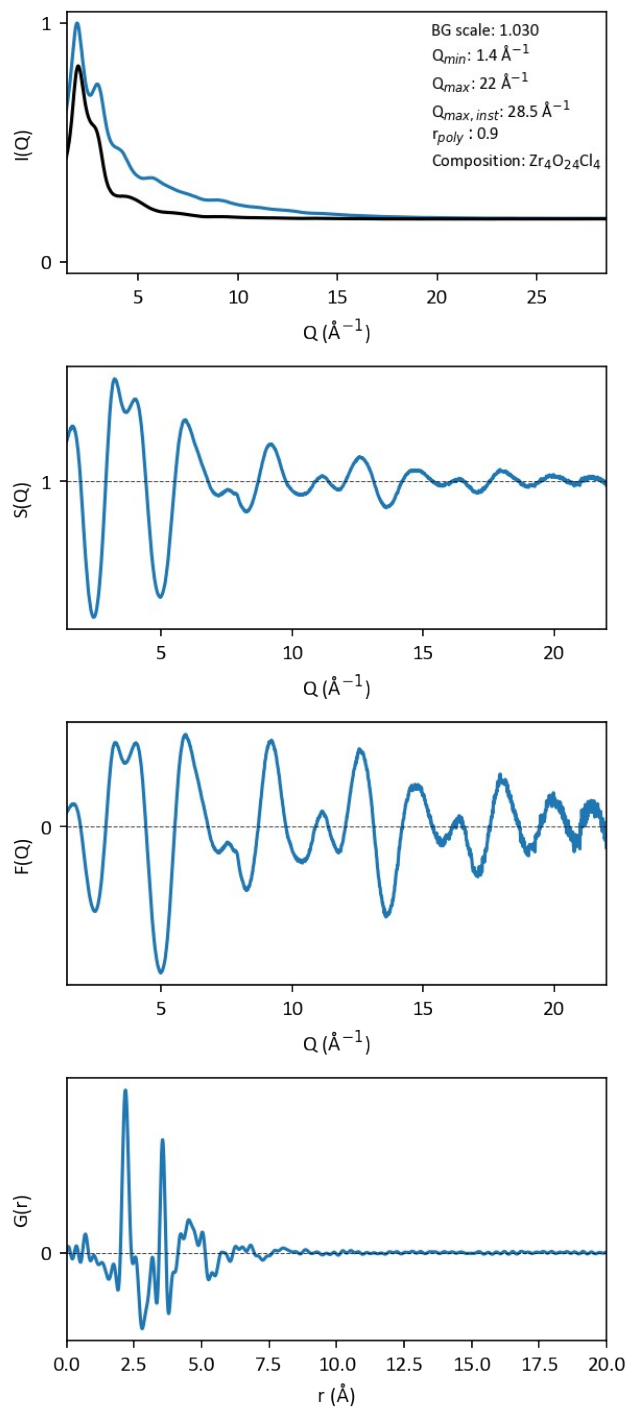


Figure S32. PDF generation of $ZrCl_4$ in H_2O (1.5 M) with data collected at P21.1@PETRA-III. a) $I(Q)$ and scaled water background used for background subtraction, b) $S(Q)$, c) $F(Q)$ and d) $G(r)$. The parameters used to generate the PDF in xPDFSuite is given in the figure.

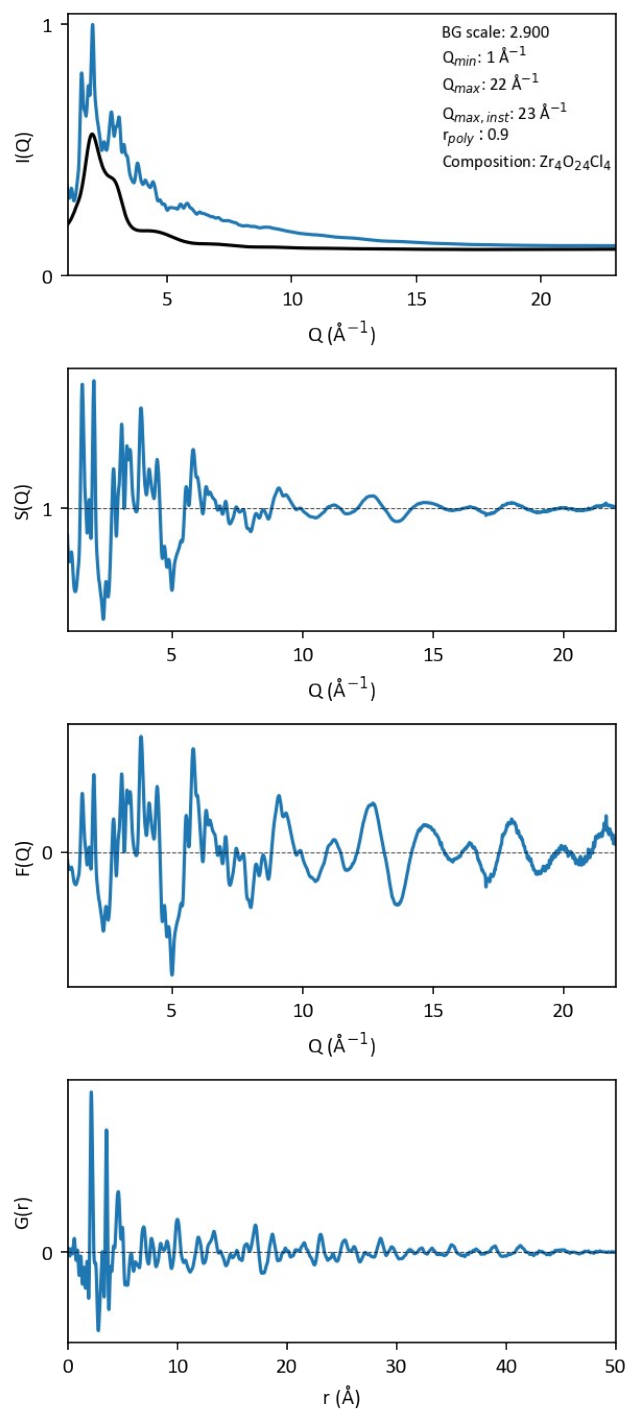


Figure S33. PDF generation of $ZrCl_4$ in H_2O (2 M) with data collected at P02.1@PETRA-III. a) $I(Q)$ and scaled water background used for background subtraction, b) $S(Q)$, c) $F(Q)$ and d) $G(r)$. The parameters used to generate the PDF in xPDFSuite is given in the figure.

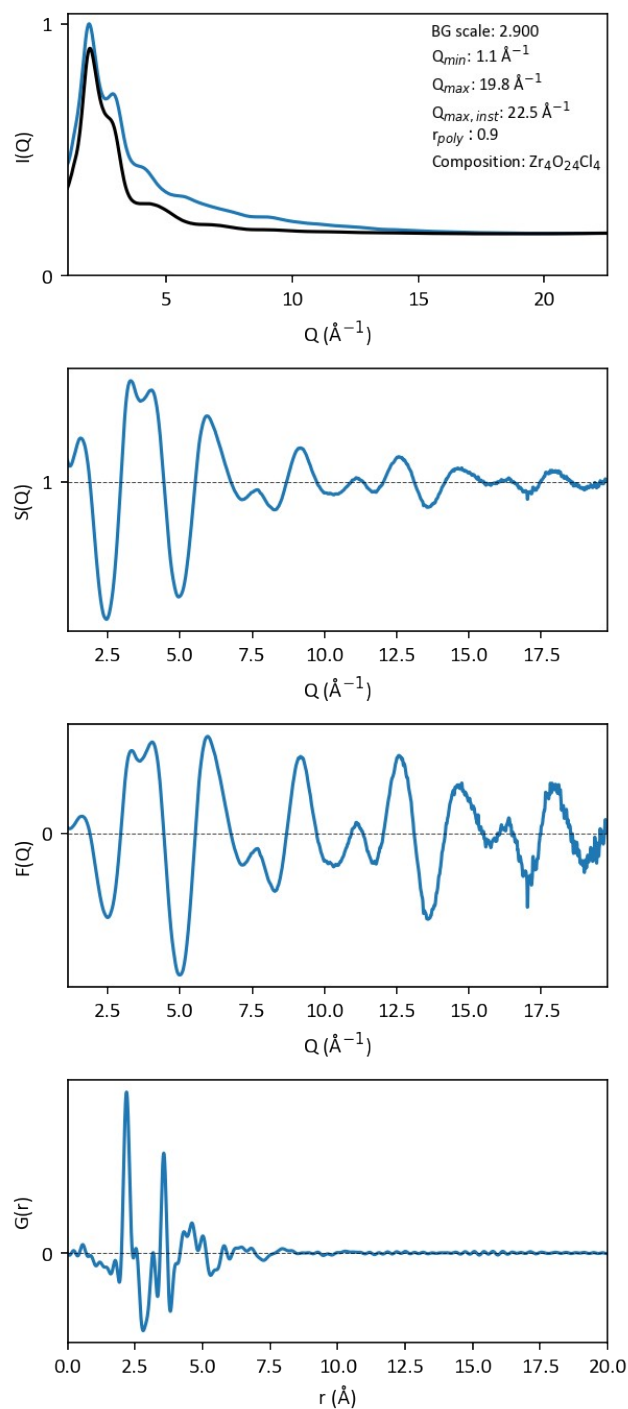


Figure S34. PDF generation of $ZrCl_4$ in H_2O (1 M) with data collected at P02.1@PETRA-III. a) $I(Q)$ and scaled water background used for background subtraction, b) $S(Q)$, c) $F(Q)$ and d) $G(r)$. The parameters used to generate the PDF in xPDFSuite is given in the figure.

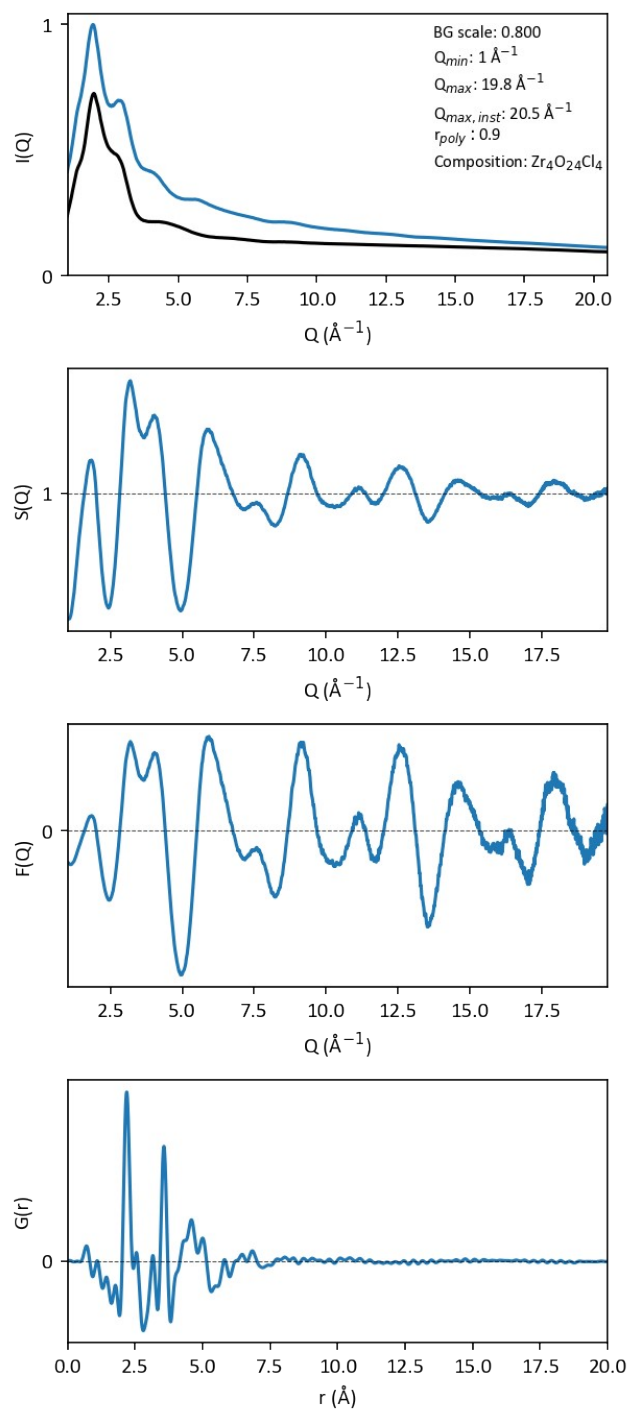


Figure S35. PDF generation of ZrCl_4 in H_2O (1 M) with data collected at DanMAX@MAX-IV. a) $I(Q)$ and scaled water background used for background subtraction, b) $S(Q)$, c) $F(Q)$ and d) $G(r)$. The parameters used to generate the PDF in xPDFSuite is given in the figure.

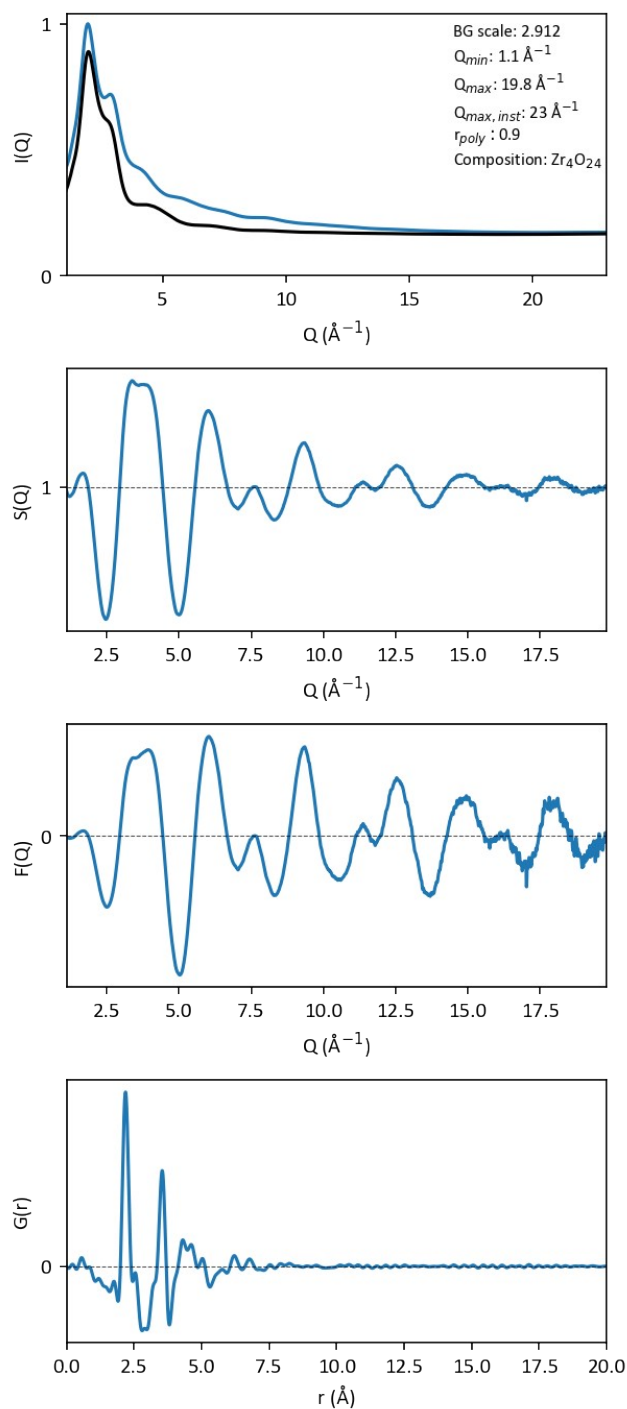


Figure S36. PDF generation of $ZrOCl_2$ in H_2O (1 M) with data collected at P02.1@PETRA-III. a) $I(Q)$ and scaled water background used for background subtraction, b) $S(Q)$, c) $F(Q)$ and d) $G(r)$. The parameters used to generate the PDF in xPDFSuite is given in the figure.

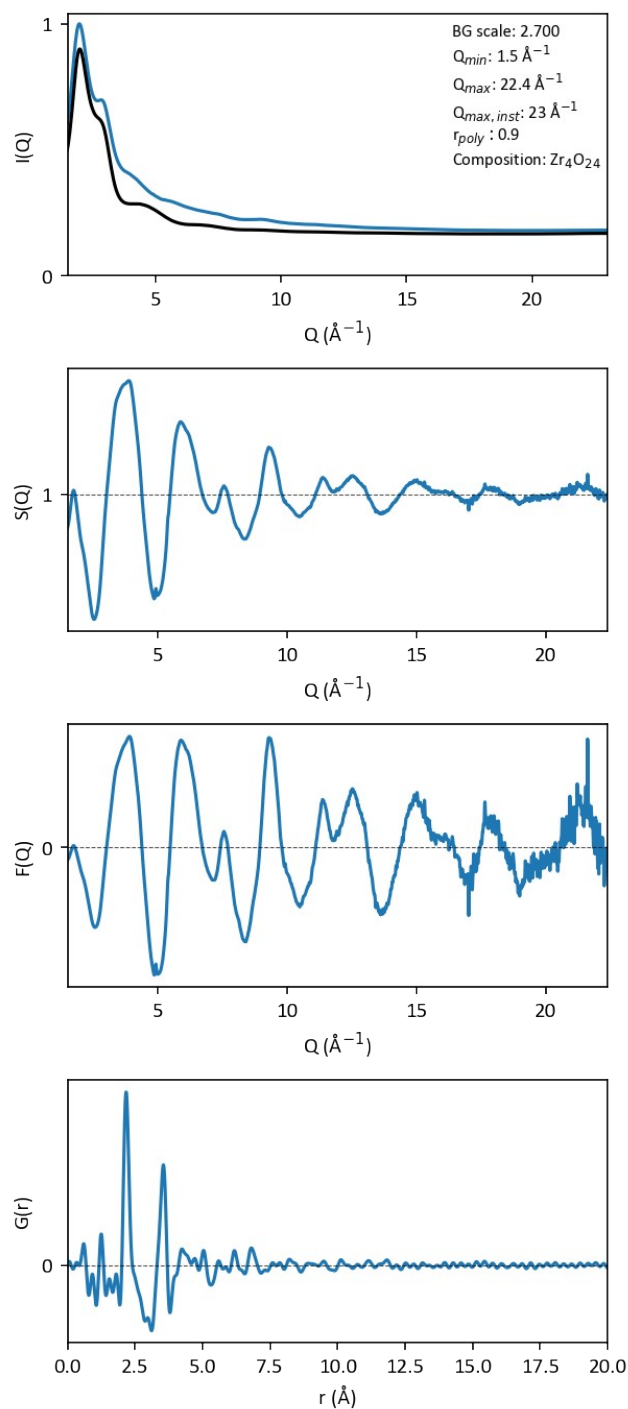


Figure S37. PDF generation of $ZrO(NO_3)_2$ in H_2O (1 M) with data collected at P02.1@PETRA-III. a) $I(Q)$ and scaled water background used for background subtraction, b) $S(Q)$, c) $F(Q)$ and d) $G(r)$. The parameters used to generate the PDF in xPDFSuite is given in the figure.

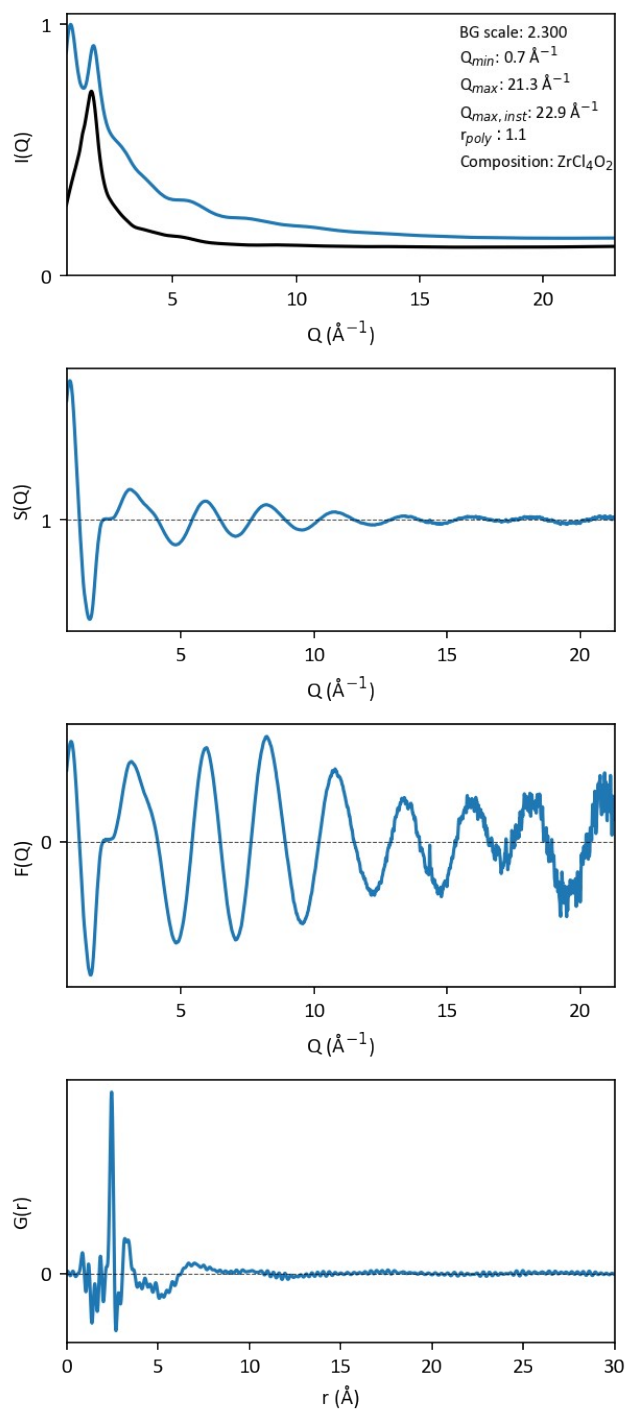


Figure S38. PDF generation of ZrCl_4 in methanol (1 M) with data collected at P02.1@PETRA-III. a) $I(Q)$ and scaled methanol+kapton background used for background subtraction, b) $S(Q)$, c) $F(Q)$ and d) $G(r)$. The parameters used to generate the PDF in xPDFSuite is given in the figure.

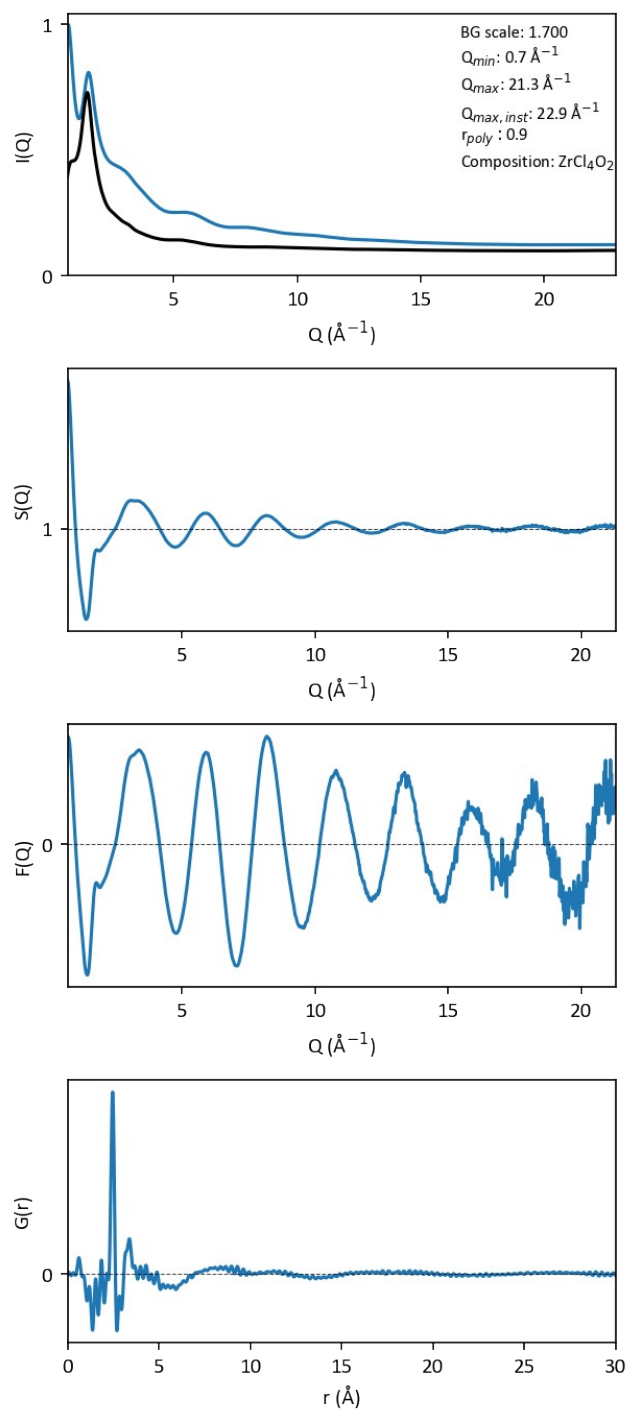


Figure S39. PDF generation of ZrCl_4 in ethanol (1 M) with data collected at P02.1@PETRA-III. a) $I(Q)$ and scaled ethanol background used for background subtraction, b) $S(Q)$, c) $F(Q)$ and d) $G(r)$. The parameters used to generate the PDF in xPDFSuite is given in the figure.

References

1. Mak, T. C. W. Refinement of the crystal structure of zirconyl chloride octahydrate. *Can. J. Chem.* **46**, 3491–3497 (1968).
2. Zobel, M., Neder, R. B. & Kimber, S. A. J. Universal solvent restructuring induced by colloidal nanoparticles. *Science* **347**, 292–294 (2015).
3. Anker, A. S. *et al.* Structural Changes during the Growth of Atomically Precise Metal Oxide Nanoclusters from Combined Pair Distribution Function and Small-Angle X-ray Scattering Analysis. *Angewandte Chemie* **133**, 20570–20579 (2021).
4. Krebs, B. Die Kristallstruktur von Zirkoniumtetrachlorid. *Z. Anorg. Allg. Chem.* **378**, 263–272 (1970).
5. Prescher, C. & Prakapenka, V. B. *DIOPTAS*: a program for reduction of two-dimensional X-ray diffraction data and data exploration. *High Pressure Res.* **35**, 223–230 (2015).
6. Yang, X., Juhas, P., Farrow, C. L. & Billinge, S. J. L. xPDFsuite: an end-to-end software solution for high throughput pair distribution function transformation, visualization and analysis. *arXiv:1402.3163 [cond-mat.mtrl-sci]* (2015).
7. Juhás, P., Davis, T., Farrow, C. L. & Billinge, S. J. L. *PDFgetX3*: a rapid and highly automatable program for processing powder diffraction data into total scattering pair distribution functions. *J. Appl. Crystallogr.* **46**, 560–566 (2013).
8. Juhás, P., Farrow, C. L., Yang, X., Knox, K. R. & Billinge, S. J. L. Complex modeling: a strategy and software program for combining multiple information sources to solve ill posed structure and nanostructure inverse problems. *Acta Crystallogr. A* **71**, 562–568 (2015).